Emplacement of monogenetic lava flows on eroded terrain, Part II: The case of the Artière valley (Grave Noire, France)

Andrew Harris, Benjamin Latutrie, Benjamin van Wyk de Vries, Élodie Saubin, Marine Foucher, Lucia Gurioli, Elena Zanella, Etienne Médard, François Nauret

Highlights

The Grave Noire lava flows extended from steep onto flat of a UNESCO World Heritage site

Facies analysis allows association of topographic effects and flow field morphology

At the break in slope at the base of a fault scarp, a perched pond was formed

The pond slowly leaked to feed slow moving, outgassed flow that excavated its substrate

Slope & type basement play fundamental roles in system architecture at monogenetic fields

Figure 1

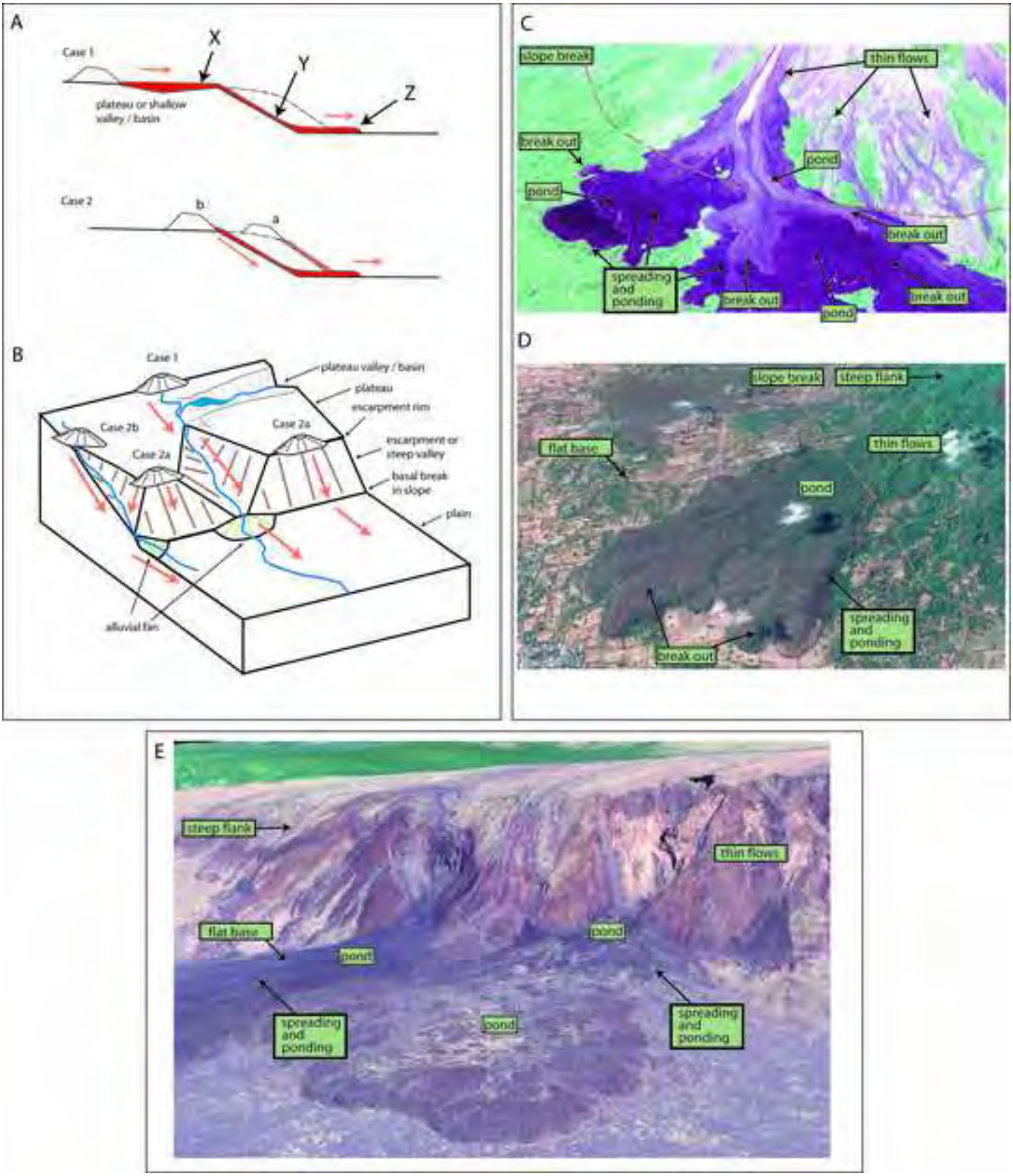

Figure 2

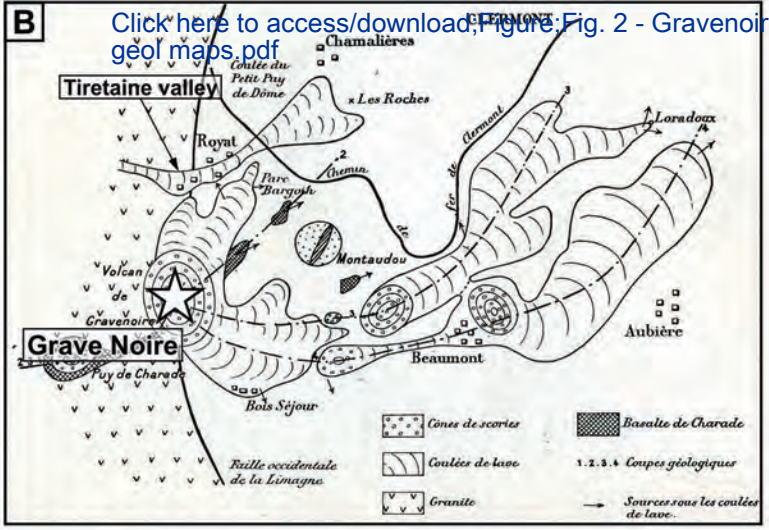

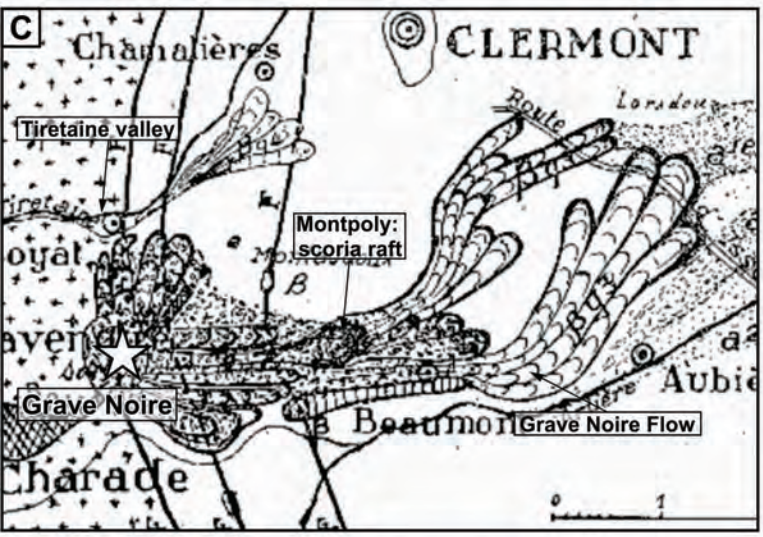

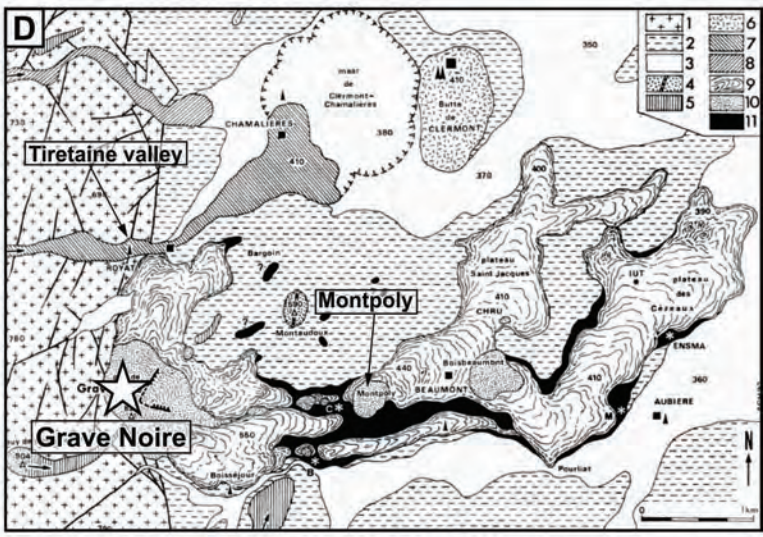

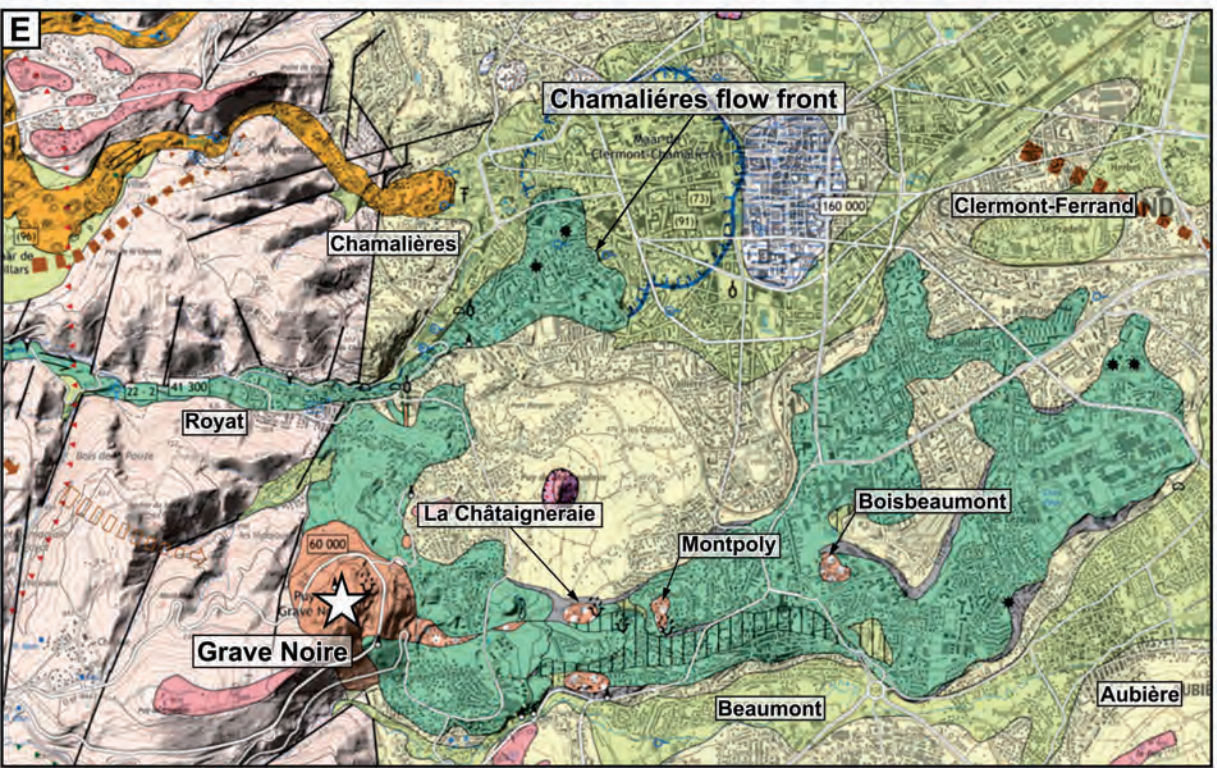

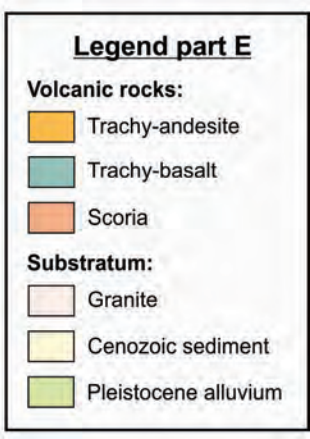

Figure 3

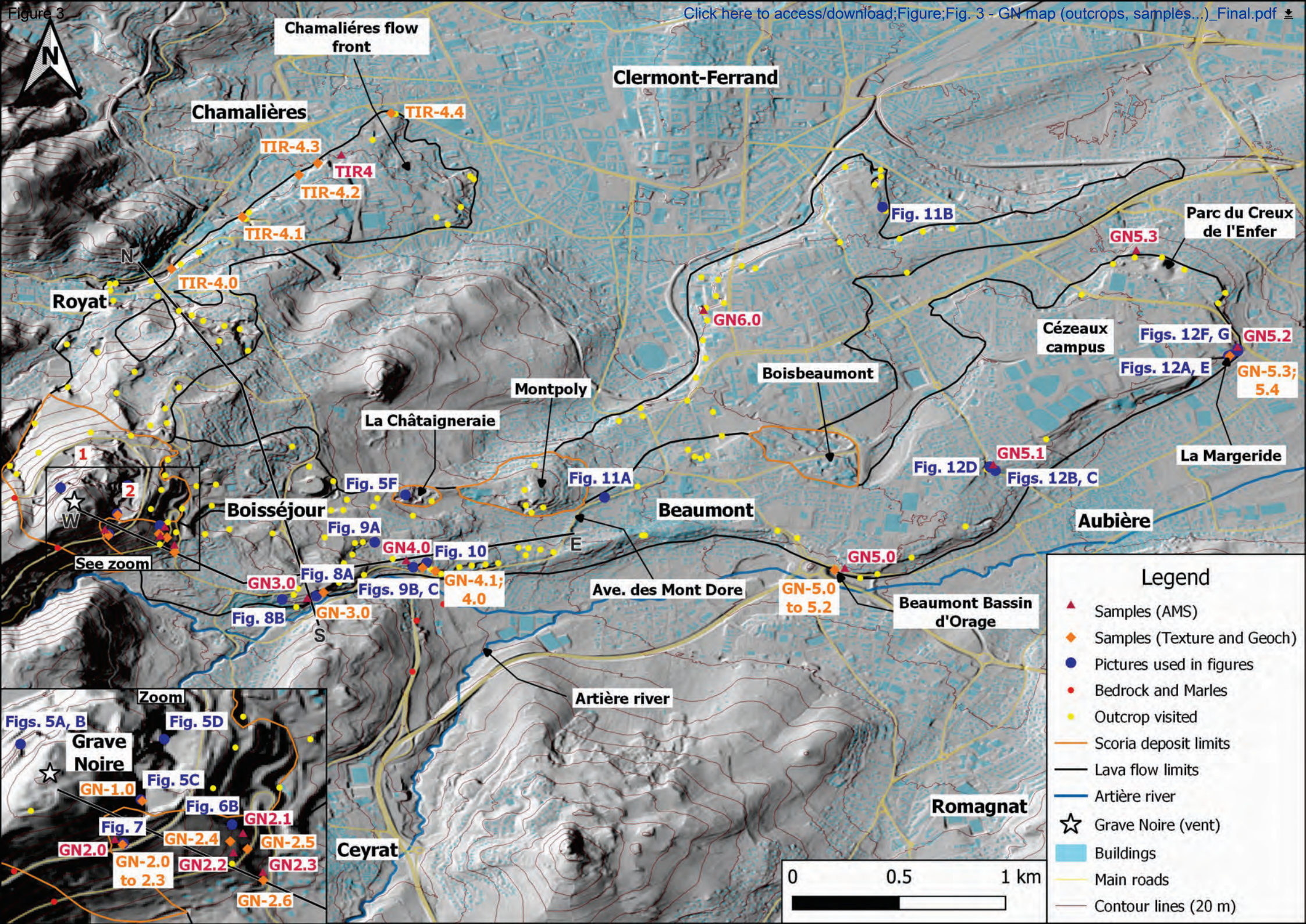

Figure 4

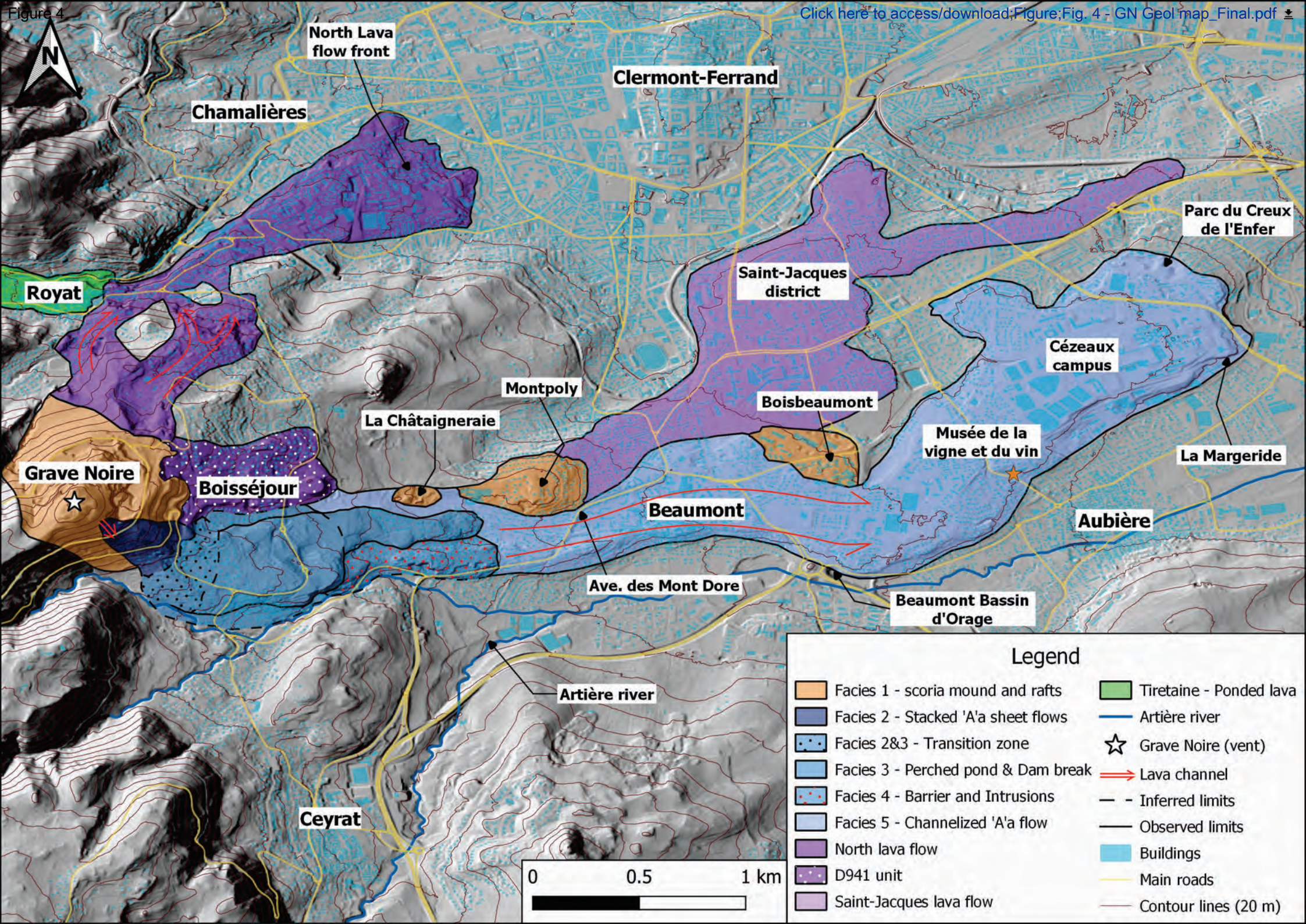

Figure 5

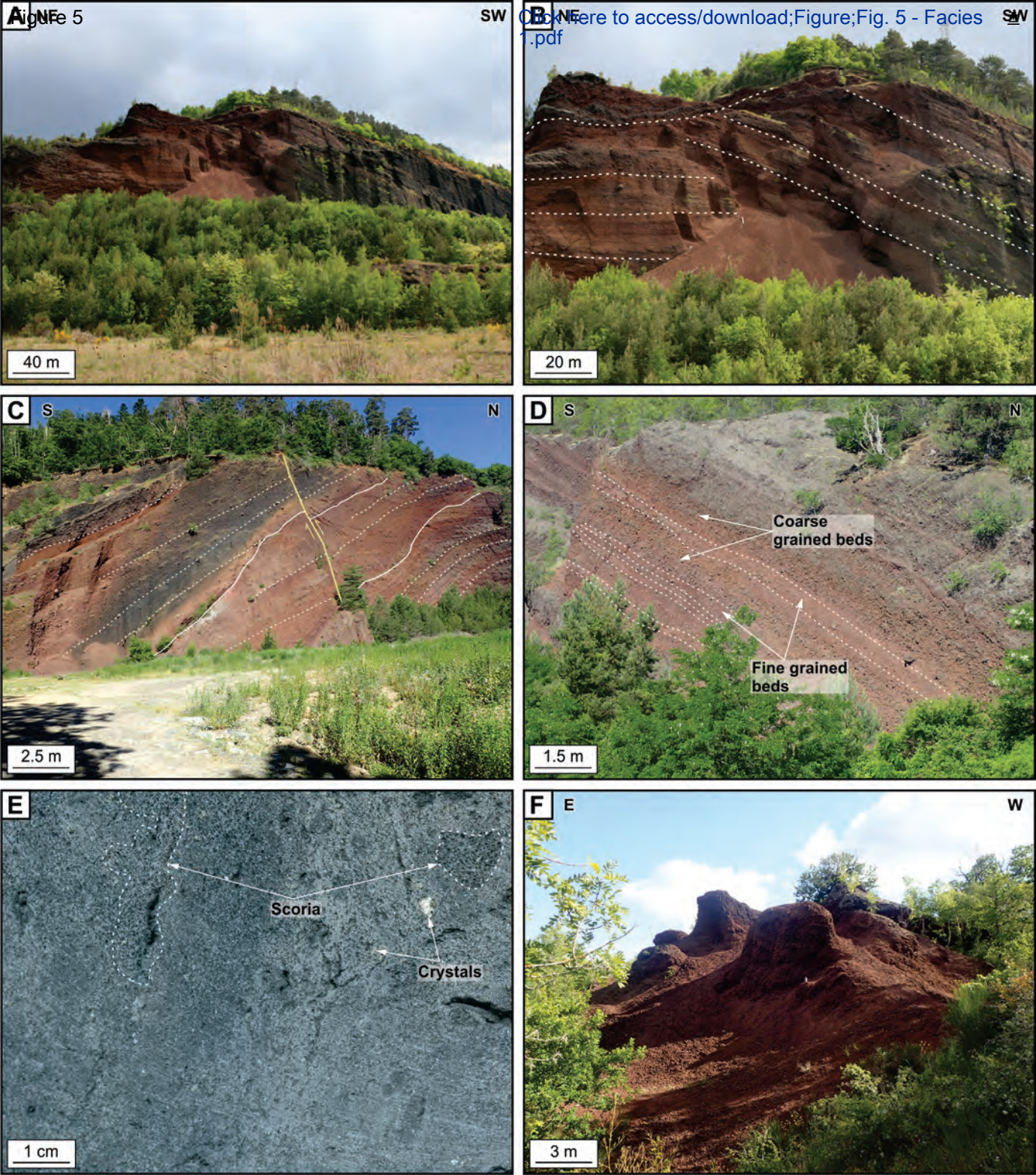

Figure 6

Click here to access/download;Figure;Fig. 6 - Facies 2 - Stacked flows.pdf

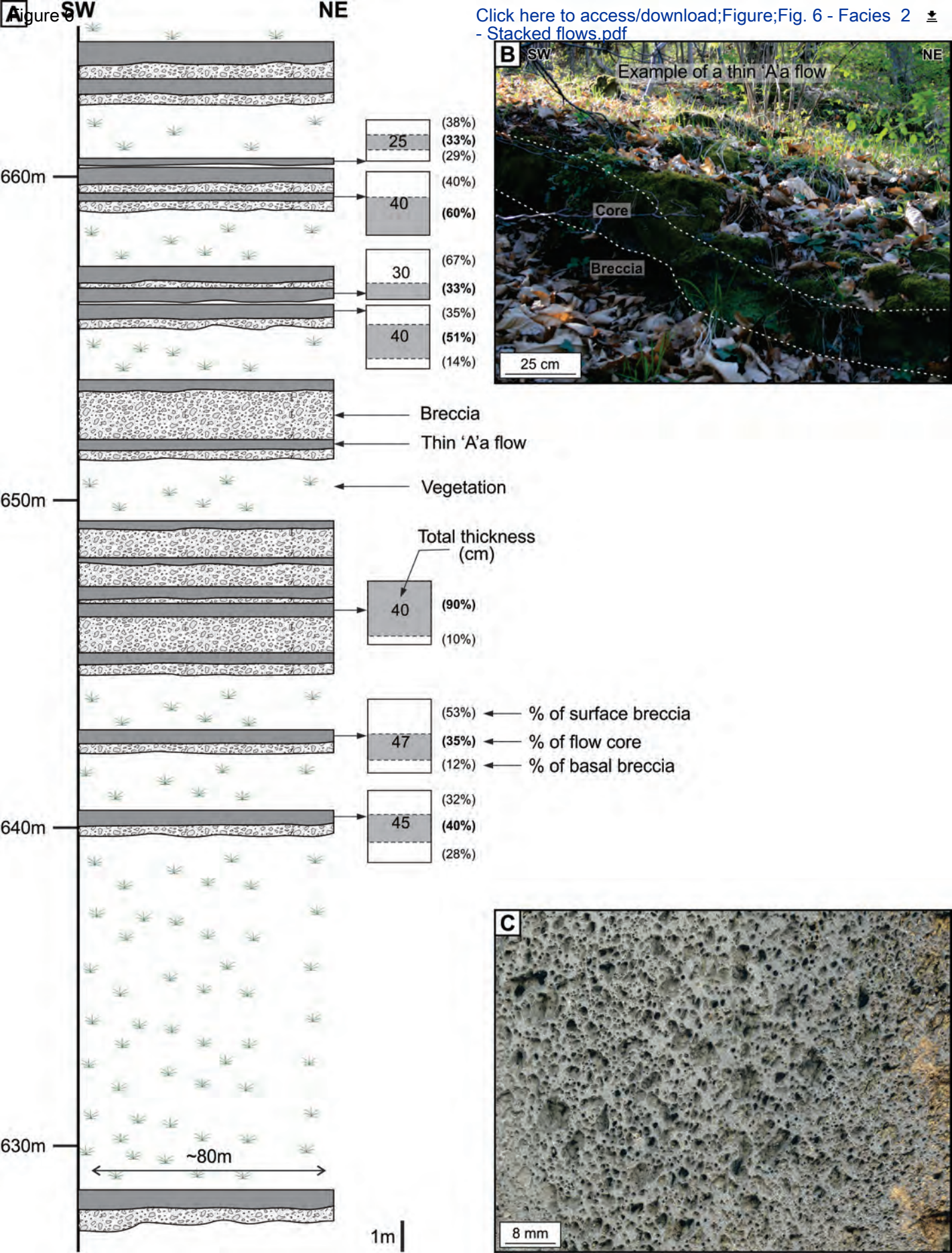

Figure 7

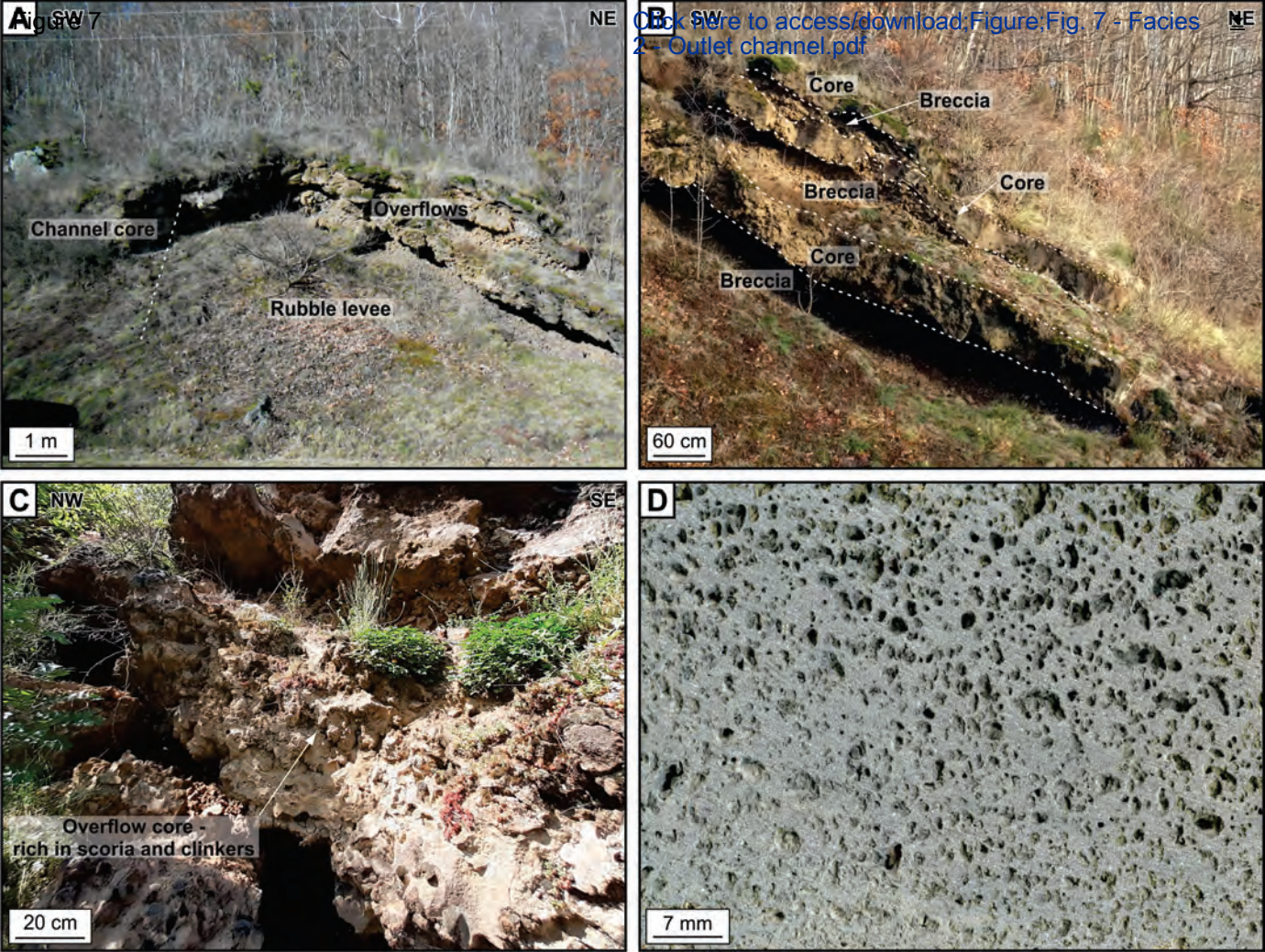

Figure 8

Click here to access/download;Figure;Fig. 8

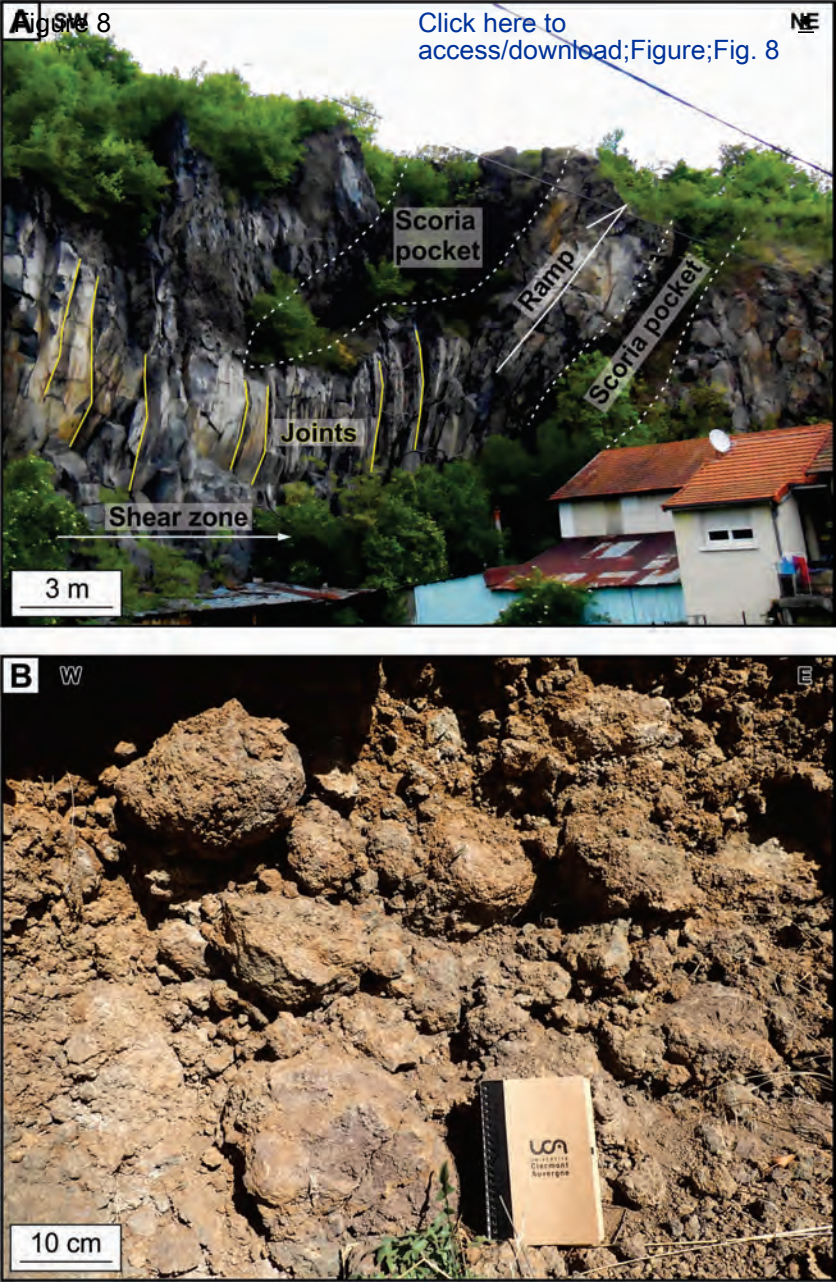

Figure 9

Click here to access/download;Figure;Fig. 9 - Facies 4 - Barrier.pdf

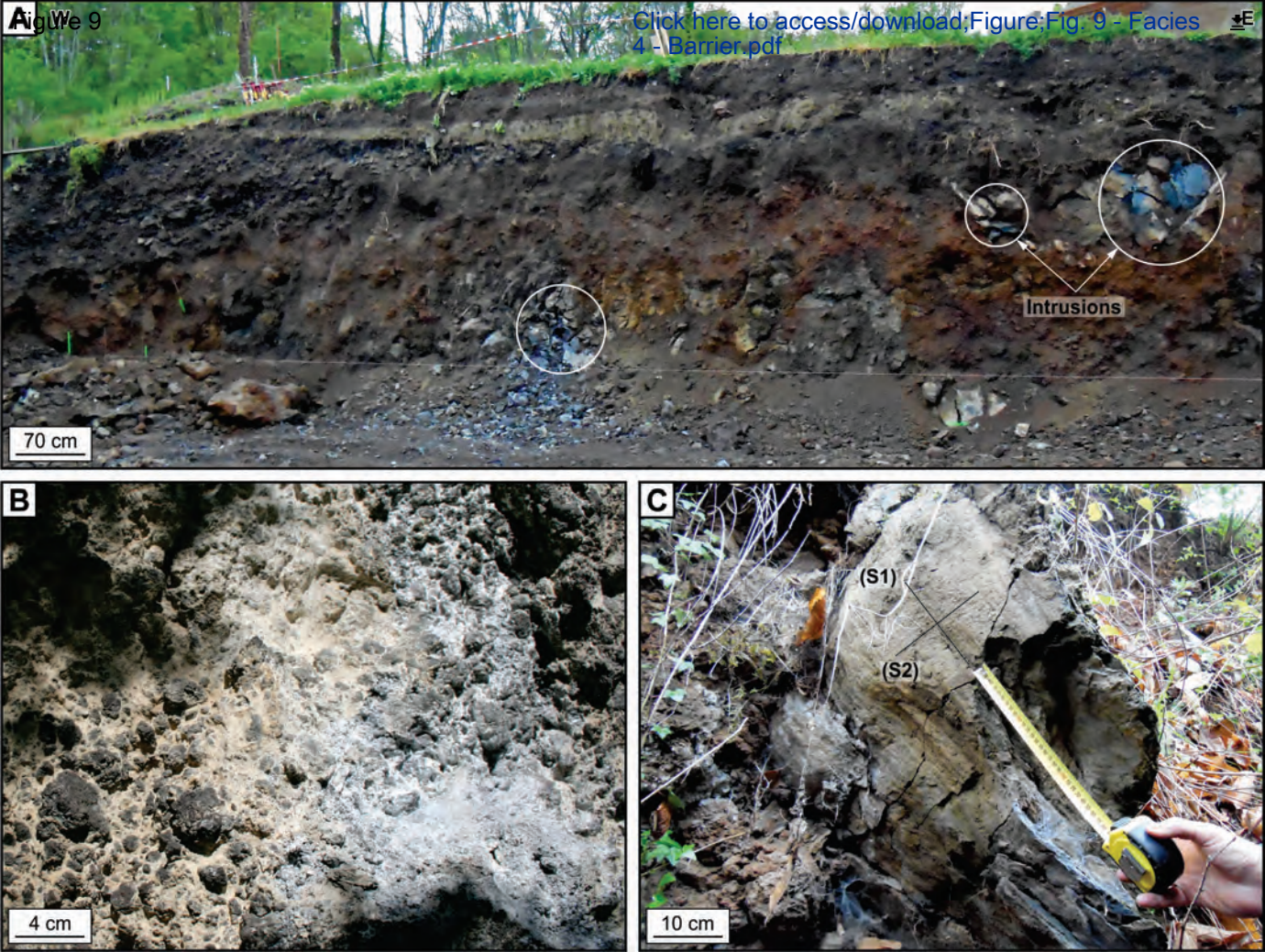

Figure 10

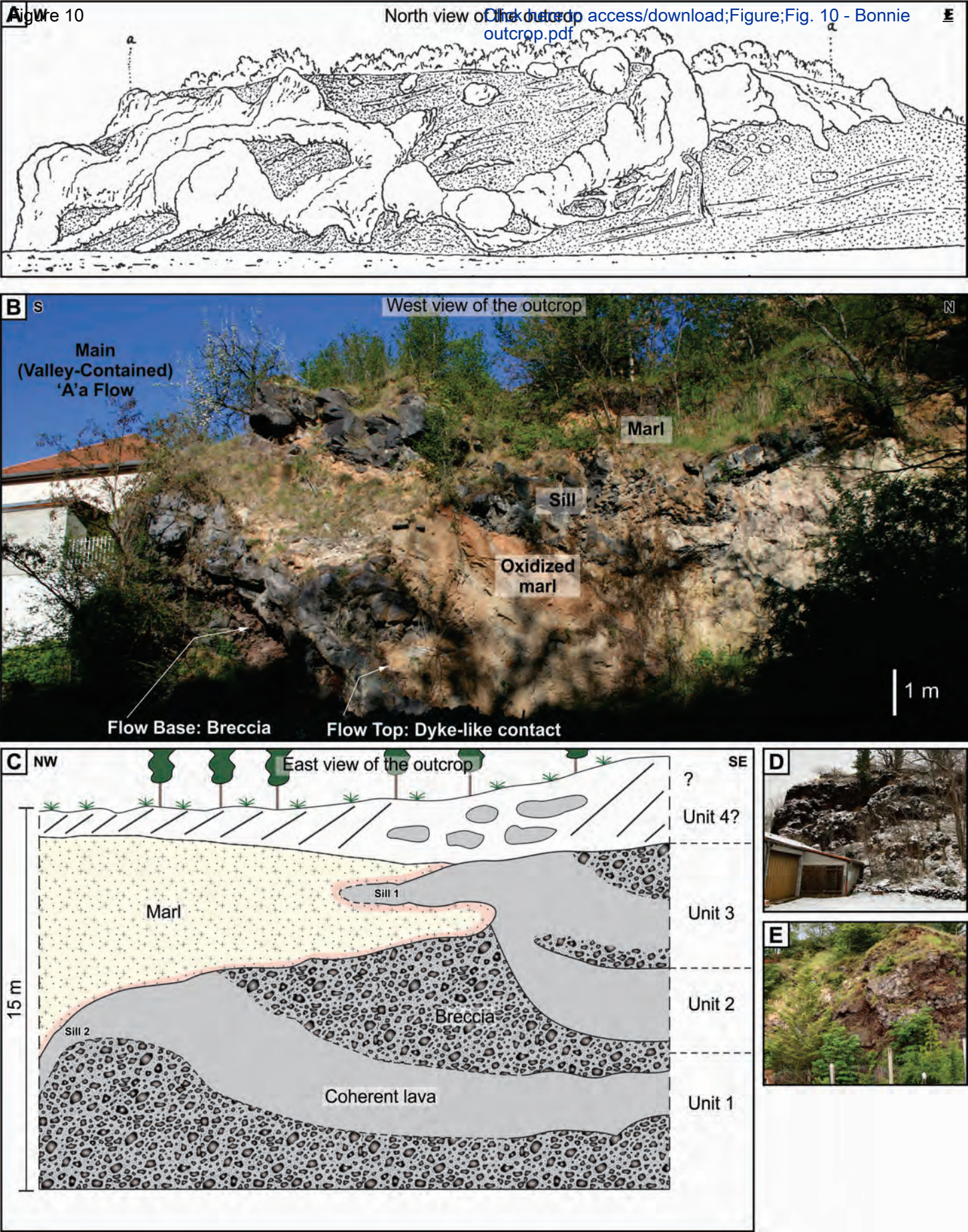

Figure 11

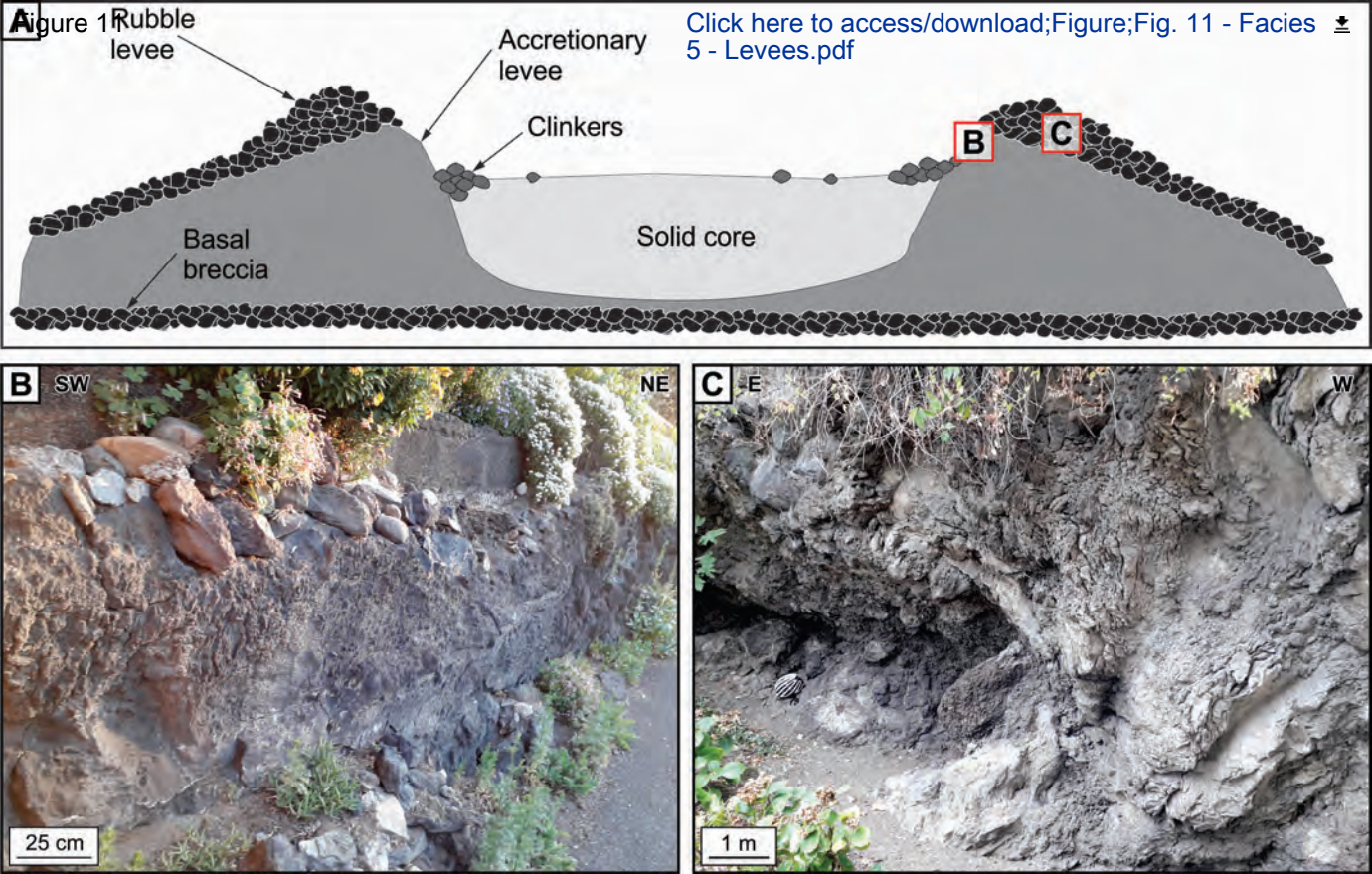

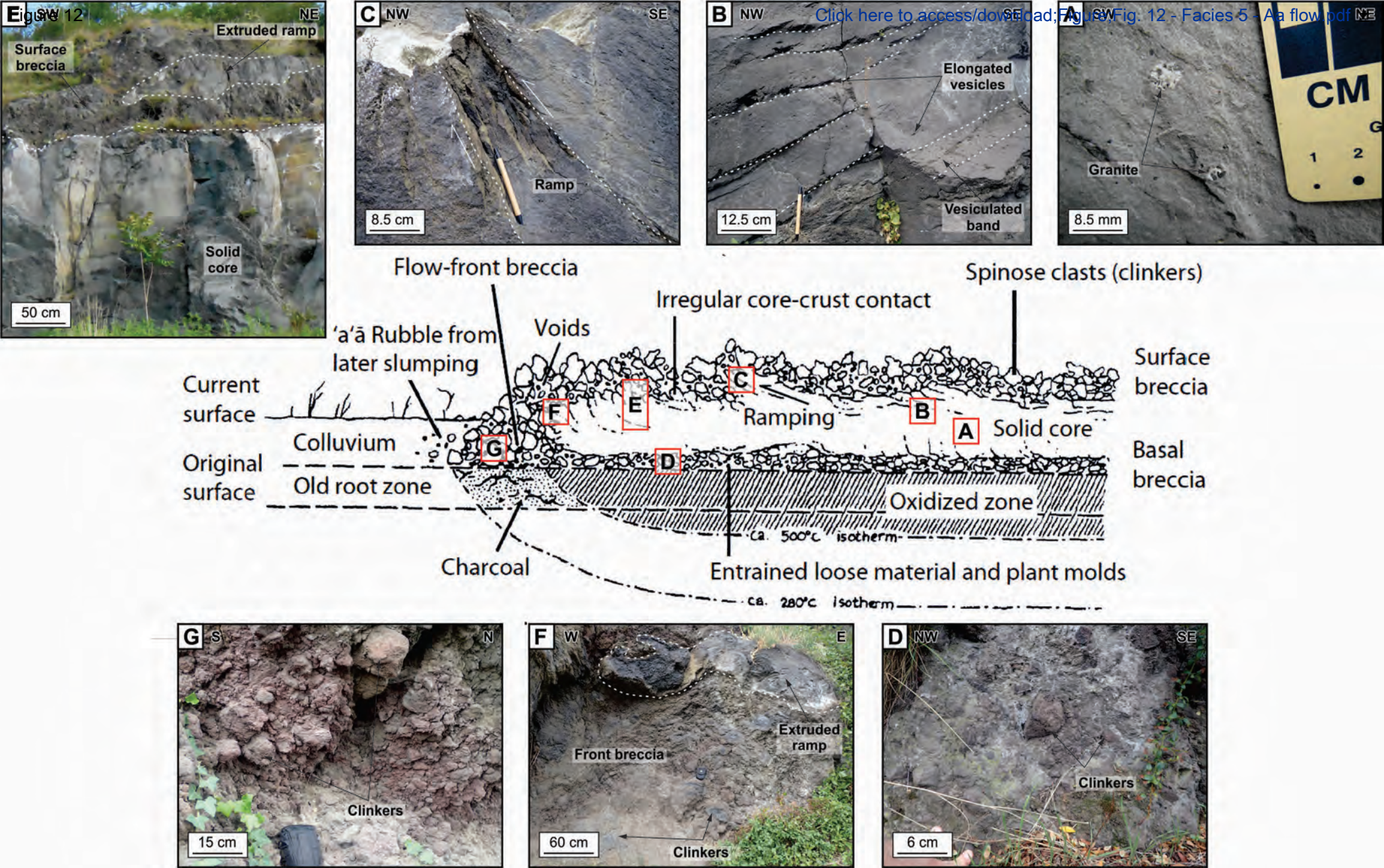

Figure 13

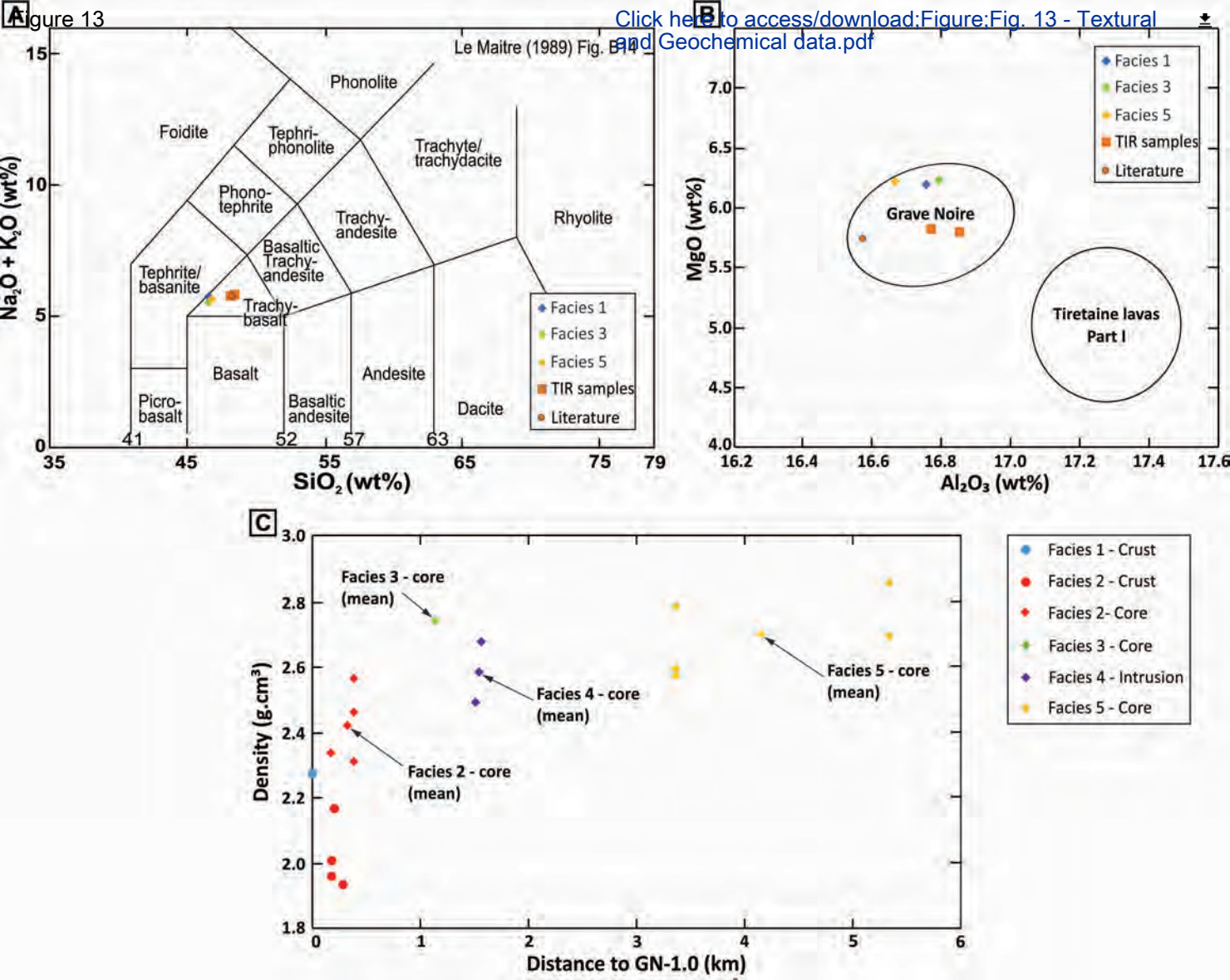

Figure 14

Click here to access/download;Figure;Fig. 14 - AMS.pdf

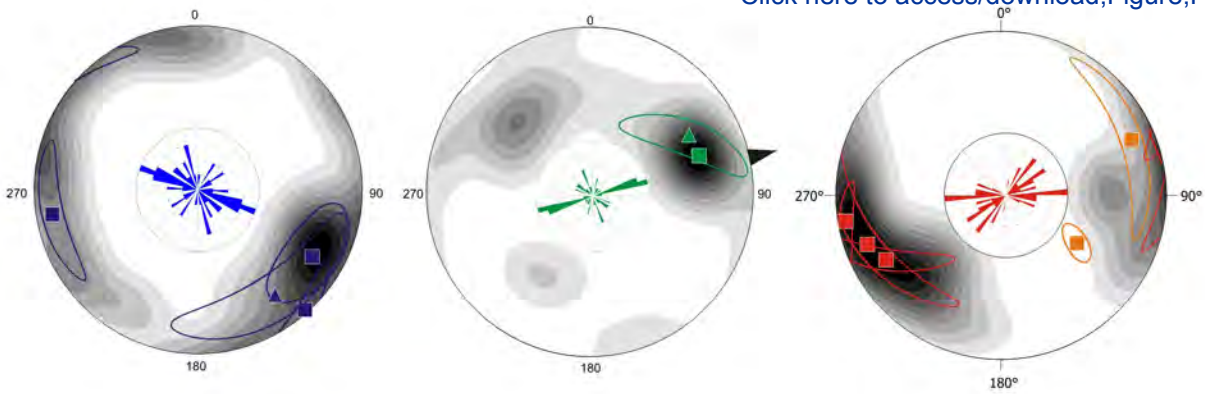

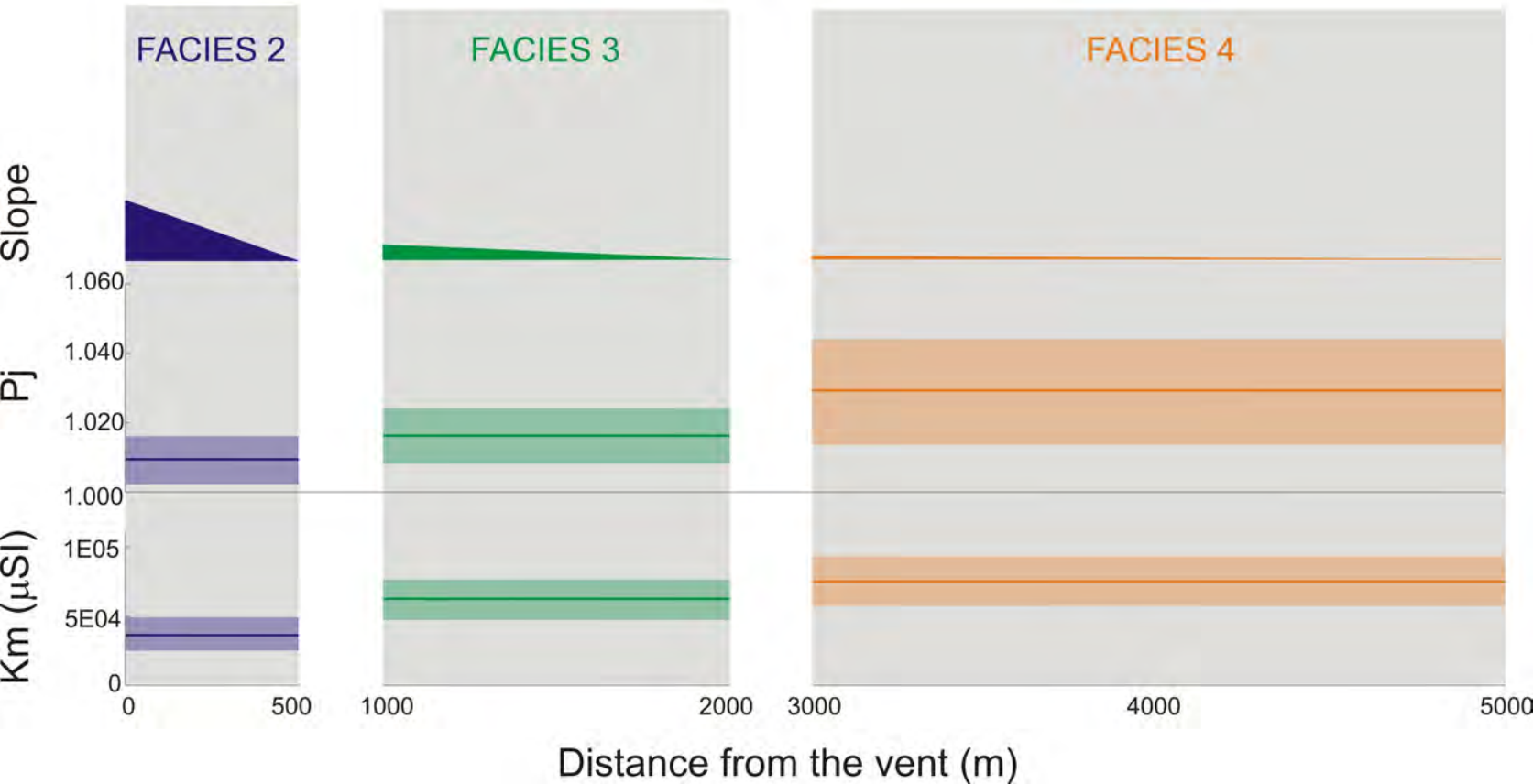

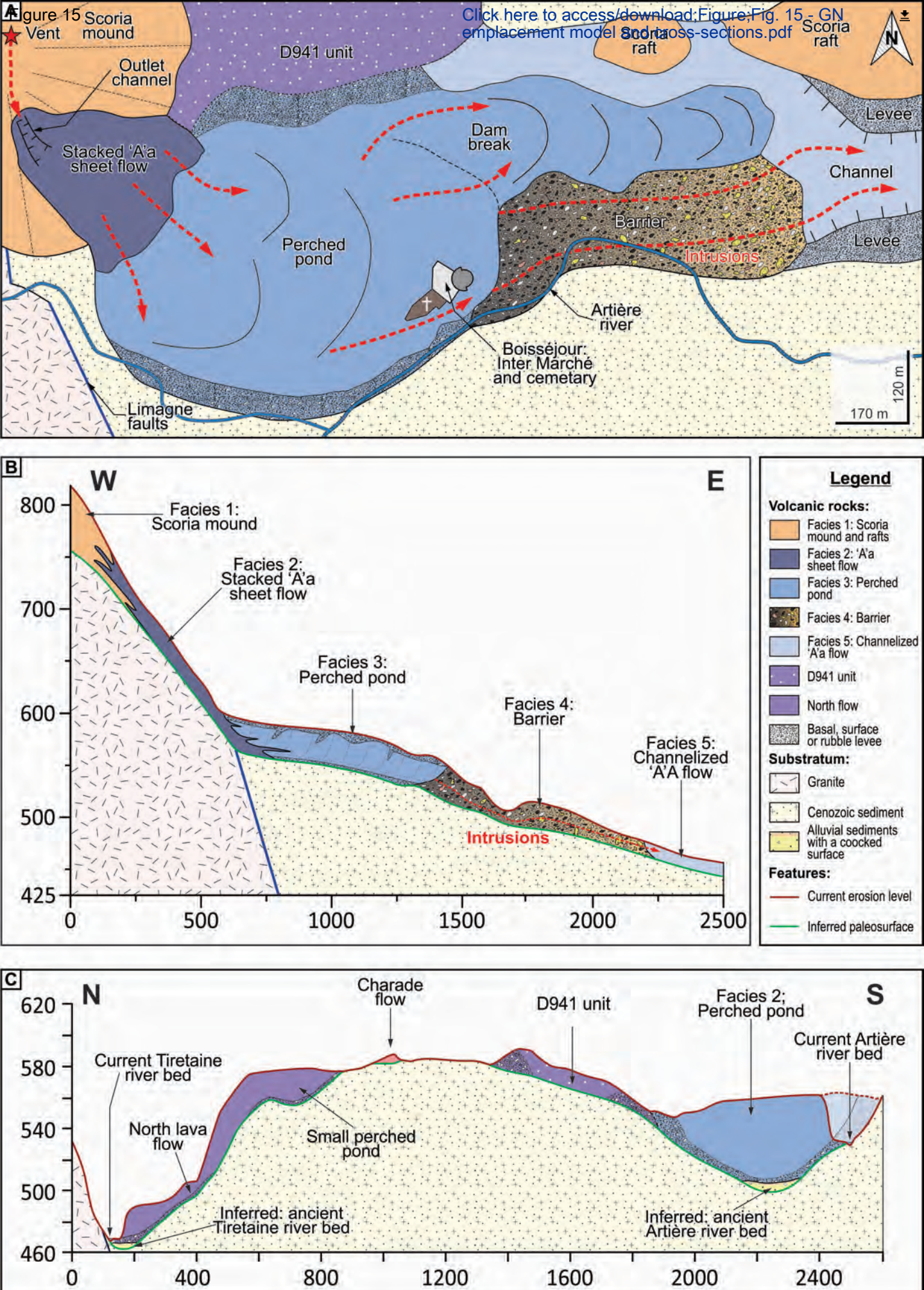

Figure 15

Figure 16

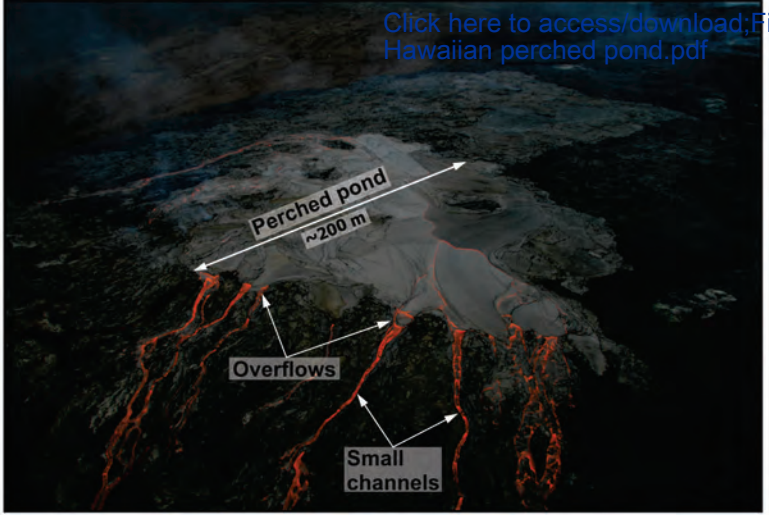

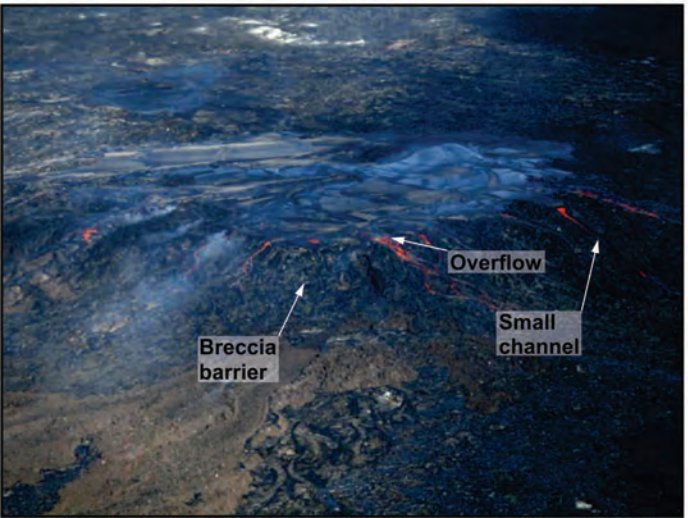

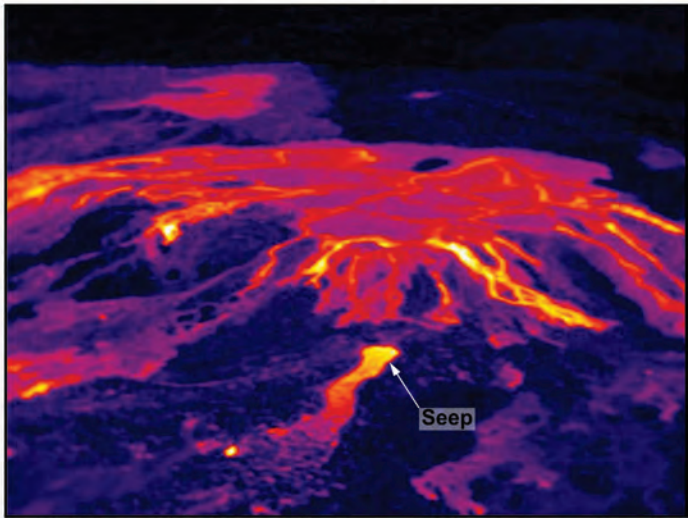

Table 1 Textural parameters calculated for the five facies of the Artière-Cézeaux lava flow, as well as for the north lava flow.

Sample name[1]	Sample type	Distance to sample GN-1.0 (km)	Archimedes' method		Point counts				
			Density (kg/cm^3)	Vesicularity (%)	N_{eff}[2] (Nb)	Crystals (%)	Stdev[3] (1σ)	Vesicularity (%)	Stdev[3] (1σ)
Facies 1:									
GN-1.0	**East quarry dyke**	**0.00**	**2290**	**22**	**105**	**3**	**1.6**	**11**	**3.1**
Facies 2:									
GN-2.0	Outlet channel - Overflow	0.17	2010	32	-	-	-	-	-
GN-2.1	Outlet channel - Overflow		1670	43	-	-	-	-	-
GN-2.2	Outlet channel - Overflow		1960	33	-	-	-	-	-
GN-2.3	Outlet channel - Core		2340	21	153	3	1.4	17	3.1
GN-2.4	Stacked flow - crust	0.20	2170	26	-	-	-	-	-
GN-2.5	Stacked flow - crust	0.28	1940	34	-	-	-	-	-
GN-2.6	Stacked flow - core	0.38	2460	16	-	-	-	-	-
GN-2.7	Stacked flow - core		2560	13	-	-	-	-	-
GN-2.8	Stacked flow - crust		1740	41	-	-	-	-	-
GN-2.9	Stacked flow - core		2310	21	13	1	3.2	0.4	1.75
Mean crust		-	1910	35	-	-	-	-	-
Mean core		-	2420	18	-	2	1.6	9	3.1
Mean Facies 2		**-**	**2120**	**24**	**-**	**2**	**2.2**	**5.7**	**3.6**
Facies 3:									
GN-3.0	**Lava lake - core**	**1.13**	**2740**	**7**	**118**	**2**	**1.2**	**16**	**3.35**
Facies 4.									
GN-4.0	Lava - intrusion	1.56	2680	9	9	1	3.6	0	-
GN-4.1	Lava - intrusion	1.50	2490	15	-	-	-	-	-
Mean Facies 4		**-**	**2580**	**12**	**9**	**1**	**3.6**	**0**	**-**
Facies 5:					-	-	-	-	-
GN-5.0	'a'ā flow - core	3.36	2780	5	-	-	-	-	-
GN-5.1	'a'ā flow - core		2590	12	-	-	-	-	-
GN-5.2	'a'ā flow - core		2570	13	-	-	-	-	-
GN-5.3	'a'ā flow - core	5.33	2850	3	-	-	-	-	-
GN-5.4	'a'ā flow - core		2690	8	-	-	-	-	-
Mean Facies 5		**-**	**2700**	**8**	**-**	**-**	**-**	**-**	**-**
North lava flow									
TIR-4.0	'a'ā flow - core	-	2500	16	93	3	1.8	9	3.0
TIR-4.1	'a'ā flow - core	-	2690	9	-	-	-	-	-
TIR-4.2	'a'ā flow - core	-	2680	9	-	-	-	-	-
TIR-4.3	'a'ā flow - core	-	2610	12	-	-	-	-	-

TIR-4.4	‘a‘ā flow - core	-	2690	9	33	1	2	3	3.0
Mean North lava flow		**-**	**2630**	**11**	**-**	**2**	**2**	**6.2**	**3.0**

[1]Location of samples is provided in Figure 3.

[2]N_{eff} correspond to the number of point that were counted both in crystals (micro-phenocrysts and phenocrysts) and in vesicles.

[3]1σ Standard deviation estimated from the equation proposed by van der Plas and Tobi (1965) based on the proportion of crystals and vesicles and the effective number (N_{eff}) proposed by Ross et al. 2021.

Table 2 Raw data of the major elements analyses (in wt%) made on three facies of the Artière-Cézeaux lava flow and two samples from the North lava flow

	Facies 1	Facies 3	Facies 4	North Flow	
Sample name[1]	GN-1.0	GN-3.0	GN-5.3	TIR-4.1	TIR-4.4
Sample type	Lava bomb	Lava lake - core	‘a‘ā flow - Core	‘a‘ā flow - Core	‘a‘ā flow - Core
SiO_2	46.36	46.26	46.64	47.99	47.48
Al_2O_3	16.57	16.57	16.52	16.50	16.50
Fe_2O_3	12.30	12.20	12.26	11.23	11.29
MgO	6.12	6.14	6.16	5.72	5.68
CaO	9.49	9.64	9.58	9.04	9.13
Na_2O	4.06	3.90	3.82	3.99	3.70
K_2O	1.65	1.62	1.82	1.79	2.00
TiO_2	2.61	2.63	2.59	2.34	2.38
MnO	0.20	0.21	0.21	0.19	0.19
P_2O_5	0.76	0.74	0.73	0.73	0.71
Ba	0.0587	0.0599	0.0603	0.0668	0.0660
Sr	0.0814	0.0827	0.0828	0.0823	0.0837
H_2O+	0.25	0.17	0.12	0.20	0.10
H_2O-	-0.48	-0.43	0.61	-0.05	0.03
Total	100.04	99.78	99.99	99.83	99.34

[1]Location of samples is provided in Figure 3.

Table 3. Comparison of the Tiretaine and Grave Noire facies, and associated emplacement dynamics and time scales. In each case, black backgrounds denote the steepest slopes, and gray the shallowest, so that a transition from black-to-gray is a break in slope that involves an abrupt transition from steep to shallow and gray-to-black is a break in slope that involves a change from shallow to steep. White background denotes the nearly flat zone of the Limagne basin that underlies the distal sections of both systems.

System location	Tiretaine (Part 1)					Artière-Cézeaux (Part 2)				
	Slope (°)	Facies	E_r (m^3/s)	V (m/s)	Time scale	Slope (°)	Facies	E_r (m^3/s)	V (m/s)	Time scale
Vent	2.4	Vent area : buried	1-5	--	--	15	Scoria mound	40-230	--	--
Proximal	2.4	Inflated pahoehoe	1-5	$<10^{-4}$	1-5.5 years	22-25	ʻaʻā sheet flow	40-60	1.5-2.1	72 hours
Medial	6	Channelized ʻaʻā	215-315	0.7-0.9	2-3 hours	<5	Perched pond	55-60	<0.002	72 hours
Distal	6	Stagnant lava pond	215-315	0	10-11 years	0.8	Barrier & seeps	0.004-0.2	0.1	3 years
Distal	2.5-0.8	Thick, sheared 'a'a*^	--	--	--	0.5	Thick, sheared aʻā^	14-17	0.001	3 years

*This is actually the North lava flow of Grave Noire which formed a lava dam in the mouth of the Tiretaine valley behind which the Tiretaine lavas ponded (Figure 3)
^These two facies are the same as they have the same source: degassed lava from perched ponds on the north and SE sides of the Grave Noire, respectively (Figure 14c; Table 1).

Declaration of interests

☐The authors declare that they have no known competing financial interests or personal relationships that could have appeared to influence the work reported in this paper.

☒The authors declare the following financial interests/personal relationships which may be considered as potential competing interests:

Andrew Harris reports financial support was provided by French National Research Agency. Andrew Harris reports a relationship with French National Research Agency that includes: funding grants.

AH, BL, BV, ES, MF, LG, EZ, EM and FN completed all fieldwork, mapping and sampling between 2011 and 2022. AH lead final write up, with all co-authors. BL and ES performed all textural and petrological analyses under the guidance of LG in 2016 and 2020-2021, and all chemical analyses under the guidance of EM and FN. EZ completed all AMS measurements. BL completed sampling, analyses and mapping as part of a contract funded by ANR-LAVA (as managed by AH) during 2020-2021.

Appendix A - Stereo images

Supplement 1

Supplement 2

Emplacement of monogenetic lava flows on eroded terrain, Part II: The case of the Artière valley (Grave Noire, France)

Andrew Harris[1*], Benjamin Latutrie[1], Benjamin van Wyk de Vries[1], Élodie Saubin[1], Marine Foucher[1], Lucia Gurioli[1], Elena Zanella[2], Etienne Médard[1], François Nauret[1]

[1]*Université Clermont Auvergne, CNRS, IRD, OPGC, Laboratoire Magmas et Volcans, 63000 Clermont-Ferrand, France*

[2]*Dipartimento di Scienze della Terra, Università degli Studi di Torino, Via Valperga Caluso 35, 10125, Torino, Italy.*

[*]*Corresponding author*

[*]*andrew.harris@uca.fr*

Formatted: Italian (Italy)

Abstract

At the Grave Noire on the eastern edge of the Chaîne des Puys (Central France) we have a well-exposed case of lava erupted directly onto steep slopes to pass, over an abrupt break-in-slope, onto into a flat-floored basin. Erupted 60 ka ago at the head of a fault scarp, flows descended the 25° slopes of the scarp to spread into the basin at its foot. We carried out mapping and facies analysis down the main (Artière-Cézeaux) lava flow, collecting 29 samples down its 6-km length and on which we completed textural, geochemical, and Anisotropy of Magnetic Susceptibility (AMS) analyses. Results reveal four lava flow facies:

i) a near-vent zone of thin (≤ 0.6 m) ‘a‘ā sheet flow on the steep (25°) slopes of the fault scarp;
ii) a >26 m thick lobate body of outgassed lava at the foot of the fault scarp;
iii) a zone of lava-scoria breccia and marl intruded by dense, outgassed lava; and,
iv) a 20–30 m thick distal flow of outgassed lava on slopes of 0.5–0.8°.

Down flow trends in vesicularity and crystal content, as well as the AMS data, mass balance calculations and analogy with systems displaying similar facies, reveal high effusion rate (40–60 m^3/s) fountain-fed flows fed an outlet channel on the steep slopes of the fault scarp. At the break-in-slope at the foot of the scarp, flows stalled, spread and dug into the country rock (marl) to become ponded behind a self-constructed barrier of lava breccia and cone material. Lava resident in this perched pond outgassed, intruded the base of the barrier and surrounding marl, and fed seeps in the breccia barrier. Seeps fed a slow moving (0.001 m/s) plug-dominated flow of dense lava that moved a further 3.6 km, digging down into the marl substrate by at-least 15 m and carrying a mixture of lava breccia, air fall scoria, debris flow material and cone rafts all the way to the flow front. As at the Tiretaine lava flow (Part 1, Latutrie et al., 2023) we find that breaks-in-slope aid in creating a system of reservoirs and transfers. For Grave Noire, rapidly emplaced flows on steep slopes fed a zone of storage (a perched pond) at the break-in-slope at the base of a fault scarp. The pond, in turn, fed slow moving flow across the flat floor of a basin. Interaction with an easily eroded substrate led to mechanical erosion, as well as 30–40 m of inversion of topography in the 60 ky since the emplacement of the flow system. Thus, the slope and type basement on which a monogenetic lava flow field is emplaced plays a fundamental role in lava flow dynamics, emplacement style and system architecture, as well as subsequent evolution of the topography.

Key Words: ‘a‘ā sheet flow, perched pond, seeps, effusion rate, break-in-slope, lava flow dynamics

1 Introduction

In this two-part paper series we consider emplacement processes when lavas are erupted onto eroded terrain where they flow from plateaux, over steep escarpments and into basins, thus also interacting with breaks-in-slope (cf. Ollier, 1988). This is the second paper in the sequence. In the first, Latutrie et al. (2023)[1], we considered lava erupted onto gently sloping terrain then moving onto steeply sloping terrain. We looked at the dynamics and defined the evolution in down system architecture of such a lava flow field. Here, we consider the opposite case: lava erupted onto steeply terrain with flow then passing over a break-in-slope and onto gently sloping terrain. As we argued in Part 1 (Latutrie et al., 2023), the lava flow systems of the Chaîne des Puys (France) are ideal cases to examine the interaction between changing topography and lava flow field form. This is due to the marked differences in topography between the plateau of the Massif Central on which the vents are located, and the fault scarp and basin to the east down which, and into which, some of the lavas have flowed (Figure 1). Such topography is common in rift settings, and is also found on shield volcanoes and arc-based stratovolcanoes that erupt lava onto steep edifices that then pass to flat plains (Figure 1).

In Hawaii, high effusion rate fountain-fed flows have been observed to form "perched ponds" (Jackson et al., 1975; Tilling et al., 1987). Wilson and Parfitt (1993) suggested that such ponds are caused by radial spreading and stalling of the flow front to form an area in which subsequently erupted lava gathers, so that the flow becomes ponded behind a barrier created by its own stalled flow front. Lava "seeping" from the base of barriers forming around such "perched ponds" can then feed further flow (Patrick and Orr, 2012). Lava descending steep stratovolcanoes onto plains interact with the topography in a similar way, where lava accumulates at the base of the edifice, spreading behind a breccia barrier that is easily breached to form breakout lobes (Figure 1). Such a system involves, from the vent to the flow front, (i) a proximal channelized section that flows into, (ii) a medial ponded area which feeds, (iii) a distal zone of lava flow.

To examine this second topographic case we select the lava flow system fed by the Grave Noire[2] vent (Figure 2a). Fountains from the Grave Noire fed high effusion rate lava flows that were erupted directly onto the Limagne fault scarp, down which they flowed before moving out onto the Limagne plain where the city of Clermont-Ferrand, the village of Boisséjour, and the towns of Beaumont and Aubière are now located (Figure 2). The eruption emplaced a lava flow system that, today, is well exposed in outcrops from the vent to the flow front, and which has been mapped and interpreted differently between 1901 and 2017 (Figure 2). The resulting lava flow system appears similar to that expected from observed Hawaiian cases where perched ponds can form at a break-in-slope from steep to gentle which favours a stalling flow front (cf. Wilson and Parfitt, 1993). However, at the Grave Noire, unlike in the present-day Hawaiian cases, availability of outcrop due to erosion over the 60,000 years since the system was emplaced allows us to view the system in vertical section at multiple down flow locations (Figure 3). This is invaluable as it allows us to examine the structures in, and textures of, lava units comprising flows feeding the pond as well as pond-draining flow (termed "seeps" by Patrick and Orr, 2012). Although lava escaping from the pond mechanically eroded, and excavated down into, the sedimentary

[1] Hereafter "Part 1"

[2] The French words "Grave" and "Noire" translate to "bank of gravel" and "black", so that the original name for the scoria mound in English was likely "bank of black gravel"; probably reflecting its black scoria appearance and the extraction of pozzolan in two quarries in the main edifice. We see from Figure 2 that, over the years, the name of the scoria mound has evolved from "Gravenoire" to "Grave Noire". We here use the modern term (Grave Noire) as used on the IGN map sheet 2531 ET.

substrate, today the process of topographic inversion is complete so that the lava flow stands as a 30 m high plateau. Thus, building on Part 1 (Latutrie et al., 2023), this makes Grave Noire a location where a further three effusive processes and two geomorphological processes can be studied.

2 Grave Noire setting

The Grave Noire vent opened at an altitude of 820 m asl on the crest of the Limagne fault scarp (Figure 2). The Limagne fault is a major regional structure that separates the Cenozoic sedimentary rocks of the Limagne plain from the Paleozoic granite of the Plateau des Dômes (Goër de Herve et al. 1993; Merle and Michon 2001, Maccaferri et al 2015). The position of Grave Noire at the crest of the Limagne fault scarp may be related to the topographic effect of the fault block on stresses in the crust (Maccaferri et al 2015). Proximally, lava from Grave Noire flowed down the steep slopes of the fault scarp and out onto the flat plain of the Limagne. Flow towards the N and NE moved into the Tiretaine valley, before turning east where these units today underly the towns of Royat and Chamalières (Figure 2). These lava flows and their role in interacting with the Tiretaine lavas erupted 41.3 ka ago were described and considered in Part 1 (Latutrie et al., 2023). Flows moving east fed a longer branch that today underlie the towns of Boisséjour[3], Beaumont and Aubière, as well as the Cézeaux campus of the *Université Clermont Auvergne*, displacing the course of the Artière stream to the south (Figure 3). This southern lava flow field can be split into two main lava flows: the Saint-Jacques flow to the north and the Artière-Cézeaux flow to the south (Figure 4). The Artière-Cézeaux lava flow is the now focus of second part of our study.

The Grave Noire eruption is dated at around 60 ka (Goër de Herve et al. 1993) and has been studied since the 18th and 19th centuries (Guettard 1752; Scrope 1858; Lecoq 1867; Pommerol 1880; Bonney 1912). The source of the Artière-Cézeaux lava flow has been debated since Glangeaud (1901) who proposed emplacement by an eruption involving five scoria cones of which the Grave Noire was the western-most (Figure 2b). Instead, Garde (1942) hypothesized that Glangeaud's (1901) "scoria cones" were disrupted parts of the Grave Noire cone that had travelled on the top of the Saint-Jacques and Artière-Cézeaux lava flows (Figure 2c). Instead, Goër de Herve et al. (1993) introduced the idea that a debris avalanche from the Grave Noire explains the deposits of mixed cone fragments, lava and marl found downslope from the source (Figure 2d). Boivin et al. (2017) thus mapped the "scoria cones" of Glangeaud (1901) as a "*debris-avalanche deposit from Puy de Grave Noire including parts of the cone*" (Figure 2e).

3 Methodology

Field and laboratory methods used were the same as described in Part 1 (Latutrie et al., 2023), where the basis of our methodology was a facies analysis following Cas and Wright (1984), with application of the lava flow facies guidelines given by Self et al. (1998) and Thordarson and Self (1998). Fieldwork was conducted between 2012 to 2016 during the Master's theses of Foucher (2013) and Saubin (2014), with descriptions being completed in 2020 and 2022. During mapping all available outcrops were visited, as located in Figure 3. Being an active urban environment, outcrops are being created and filled nearly constantly as part of construction work.

[3] We see from Figure 2 that, over the years, while the name of the scoria mound has evolved from one word (Gravenoire) to two (Grave Noire), the name of the town "Boisséjour" has evolved from two words to one. Again, we here use the modern term (Boisséjour) as used on the IGN map sheet 2531 ET.

Our observations of two key sites that temporally exposed the channel-substrate contact and flow front during laet 2022 and early 2023 are given in Supplements 1 and 2, respectively.

Five facies were mapped across the Artière-Cézeaux lava flow system, Facies 1 being proximal and Facies 5 being distal (Figure 4). We collected 19 samples distributed between the five facies for textural and geochemical analyses (Figure 3; Table 1). Density was measured for all samples, and five thin sections were point counted to quantify crystallinity (Table 1). Geochemical analyses were completed for Facies 1, 3 and 4. (Table 2), and drill cores were collected for Anisotropy of Magnetic Susceptibility (AMS) measurements. For AMS, 10 samples were taken spanning all facies down the Artière-Cézeaux unit, plus one from the Saint-Jacques unit (Figure 3; Appendix A). These were used to obtain flow direction and to assess down-system trends in terms of degree of anisotropy (P_j) and magnetic susceptibility (Km).

4 Results

We can divide the Grave Noire lava flow system into four lava flows: north, D941, Saint Jacques and Artière-Cézeaux (Figure 4). The north flow moved down the south side of the Tiretaine valley before turning west to spread out over the Limagne plain and into the maar that underlies Clermont Ferrand (see Part 1, Latutrie et al., 2023). Lava that moved down the scarp to the east and south can be divided into (from north to south):

1. A poorly exposed lava flow of limited extent that we name after the departmental road (the D941) that, today, runs over the flow front. It is ~750 m long and ~250 m wide (dark purple with white stipple, Figure 4).
2. The Saint Jacques lava flow is ~6.1 km long and is up to ~800 m wide (light purple, Figure 4).
3. The Artière-Cézeaux lava flow is 5.9 km long and is up to 750 m wide. Distally it overlies the Saint Jacques lava flow, and is the lava flow on which we here focus (shades of blue, Figure 4).

Based on our analysis, the Artière-Cézeaux lava flow can be divided into five facies. These are, from the vent to the flow front: (i) scoria mound and cone chunks; (ii) thin, stacked ‘a‘ā flows; (iii) ponded lava; (iv) intruded lava-scoria breccia and marl; and (v) dense ‘a‘ā lava flow (Figure 4).

4.1. Facies 1: scoria mound and cone chunks

Facies 1 comprises the scoria mound that forms the Grave Noire (Figure 4). Grave Noire has a rounded shape, a diameter of ~700 m, is built at the head of the Limagne fault and has no crater. Thus, following Ollier (1988), it is a scoria mound. Quarries expose the interior of the mound providing sections of up to 40–50 m in height, where two quarries exposes the northwest and eastern sectors of the mound, respectively (Figure 5).

The northwest quarry exposes well-sorted beds of lapilli tuff and minor tuff breccia. Each bed is tens of centimeters to several meters thick, and is moderately-to-strongly welded (Figure 5a). Degree of welding varies with grain size, where the tuff breccia is moderately welded, and the lapilli tuff is strongly welded (Figure 5b). Beds have dips of 25–30° to the southeast, but are cut uncomformably by sub-horizontal beds (Figure 5a). Scoria deposits are black-to-dark red towards the outer flanks, changing to Bordeaux red towards the centre (Figure 5a).

The east side of Grave Noire was emplaced at the head of the steepest (25°) slopes of the Limagne fault, and structures and bedding in the east quarry are much more chaotic than in the northwest quarry, being cut by at-least three unconformities (Figure 5c). Bedding is irregular with thick (several meters) beds of coarse lapilli tuff-to-tuff breccia, and thinner (centimetres to tens-of-centimetres) beds of medium-to-coarse lapilli tuff.

Deposits alternate from black to Bordeaux red and display discordant contacts with at-least four different dips. Individual beds are sorted and grade into each other showing normal grading (Figure 5d). The exception is a zone to the south that is a 50 m thickness of unbedded but sorted black scoria with occasional bombs (Figure 5c). The welding of the east side deposits is similar to those of the northwest side. Distally, Facies 1 deposits have been reworked and/or remobilized as lahars and debris flows (e.g., at site GN2.1, Figure 3).

Two sub-vertical dykes cross-cut the scoria mound, one in each quarry. The dyke in the northwest quarry is 1.15 m wide and has a dense central plug zone surrounded by moderately vesicular sub-vertical shear zones. The dyke in the east quarry is 40 cm wide and is non-vesicular. Both dykes have 2–3% of micro-phenocrysts, plus phenocrysts of clinopyroxene and olivine of millimetric (up to 4 mm) size (Figure 5e, Table 1). Dyke xenoliths include 3 cm pieces of granite and 5 mm fragments of free quartz.

Scoria piles crop out to the east of Grave Noire, above all towards the margins of the Artière-Cézeaux unit, with the three largest being those of La Châtaigneraie, Montpoly and Boisbeaumont (Figure 4). Of these, the best outcrop is located at La Châtaigneraie (although those of Montpoly and Boisbeaumont are larger, they are covered by buildings). The scoria pile of La Châtaigneraie has a diameter of 70 m and a height of 15 m (those of Montpoly and Boisbeaumont are over 500 m across and up to 40 m high). Deposits of La Châtaigneraie pile are moderately-to-strongly welded and are composed of scoria beds of lapilli tuff lapilli tuff with minor tuff breccia. Beds are a few centimetres to a meter in thickness, and are thus identical to the deposits of the Grave Noire eastern quarry (Figure 5f). In the central part of La Châtaigneraie pile, beds are sub-horizontal with a gentle dip to the south. Fragments are mainly scoria with rare spatter, black to Bordeaux red in colour, and mainly amoeboid in shape (angular when broken). The interior of larger bombs (tens of centimetres in size) display alternation of non-vesicular (dense) to vesicular bands and granite xenoliths. Mineral content of the scoria is the same as the Grave Noire dykes, with 2–3% micro-phenocrysts and phenocrysts of clinopyroxene and olivine. Hereafter termed “cone chunks”, scoria piles of such composition, but smaller size, can be found all the way to the front of the Artière-Cézeaux flow (see Supplements 1 and 2).

4.2. Facies 2: stacked ‘a‘ā flows

Facies 2 is a stack of thin (≤0.6 m) ‘a‘ā flows and is found on the steep (~25°) slopes immediately to the southeast of Grave Noire (Figure 4). Facies 2 covers an area ~0.55 km^2, extending 0.5 km to the edge of Boisséjour where there is an abrupt decrease in slope to 5–3°. These lava flows are on the scoria deposits of Facies 1 and were first mentioned by Bournet (1957). At-least 18 lava flows can be counted (Figure 6a), with thicknesses ranging from 25 to 60 cm, with an average of 35 cm (Figure 6b). By flow thickness, each ‘a‘ā is characterized by 49% dense-to-moderately vesicular core (Figure 6c), 38% surface breccia and 13% basal breccia (Figure 6a). Based on 18 units counted, with a total combined thickness of around 17.5 m, and given a vertical distance of 35 m between the first and last exposed unit (Figure 6a), we estimate that around 40 units comprise the stack. The missing units are hidden by forest cover. These ‘a‘ā units have a crystallinity of ~2%, with olivine and clinopyroxene phenocrysts (Table 1).

‘A‘ā sheets can be traced to what appears to be an outlet channel exiting the vent area to the southeast. The left bank of the channel is well-exposed at a road cut at the southern edge of the east quarry (Figure 7a). Here three overflow levees overlie a 3.5 to 4 m high rubble levee (Figure 7b). Interiors of overflow units are 50–80 cm thick and separated by brecciated layers that are 30–50 cm thick. Interiors are rich in entrained breccia

(Figure 7c) and contain sub-rounded to slightly elongated vesicles (Figure 7d). Flow breccia is a mix of ‘a‘ā clasts and broken bombs, with rarer coarse tuff and fine lapilli tuff. Inboard of the levee, lava is dense and AMS-derived flow directions turn down slope, as opposed to tangentially away from the channel axis in the overflow units. The right bank levee is not exposed, but from the form of the outcrop we estimate the channel to have been around 7 m across.

4.3. Facies 3: ponded lava

Facies 3 is found at the break-in-slope at foot of the Limagne fault scarp (Figure 4). Here slope changes from ~25° to 5–3°. Facies 3 covers an area of ~0.4 km^2, is several tens of meters thick and comprises dense (non-vesicular) lava (Figure 8a). The main unit is lobate in form and has dimensions of 870 × 820 m (Figure 4). Across a 250 m wide “transitional” facies zone at the base of the fault scarp Facies 3 is overlain by, and inter-fingered with, units of Facies 2 (Figure 4). Both the surface and basal breccia are of irregular thickness, and contain pockets of scoria a few meters across (Figure 8b), some of which have been entrained into the dense interior of the flow (Figure 8a). Both the basal and, above all, the surface breccia are a mix of lava clinker derived from the flow itself and scoria, as well as angular blocks of dense lava. The surface breccia is typically a 50:50 mix of clinker and scoria (based on a count of 305 clasts at 19 different locations). In places we find that the breccia is 100% scoria, but it is never 100% clinker (max = 90%).

The unit is well exposed (i.e., both the basal and surface breccia are apparent) in a quarry on the southern edge of Boisséjour (GN-3.0, Figure 3). Here a 26 m thickness of dense lava is exposed (Figure 8a), with a base characterized by a 1 m thick shear zone overlying a basal breccia. Sense of shear is to the east (i.e., in the downhill direction), an orientation coherent with the AMS-derived flow direction. The unit displays poorly-formed cooling joints (columns) and ramp structures. These are also deformed to the east (Figure 8a). Around ramp structures, the surface breccia fingers down into the dense interior lava to form meter-to-decimetre sized pockets of entrained surface breccia (Figure 8a). The crystal content of Facies 3 is 2%, with phenocrysts of olivine and clinopyroxene and rare feldspar, and is identical to that of Facies 1 and 2 (Table 1).

4.4. Facies 4: intruded lava-scoria breccia and marl

Facies 4 crops out immediately east of Facies 3 (Figure 4), and is characterized by a polylithic breccia intruded by dykes and sills (Figures 9, 10). Breccia composition varies from west to east, i.e., down system. To the west breccia is of purely volcanic fragments and has the same componentry as the breccia associated with Facies 3 (Figures 8b, 9a). That is, it is a 50:50 mix of ‘a‘ā clinker and vesicular scoria with rarer angular blocks of dense lava. Exposures of breccia are 10–15 m thick. A 20 cm layer of well-sorted, black, coarse scoria overlain by a similar thickness of debris flow can be found capping the breccia in some locations. To the east, the breccia contains blocks of marl and is mixed with powdered marl (Figure 9b); marl being the basement rock of the basin onto which this facies was emplaced (Cenozoic sediments in Figure 2e). In places, especially around intrusions and for entrained cm-sized fragments of marl, the marl is oxidized and “cooked” (Borde and Rudel 1939).

The nature of the intrusions also evolves from west to east. Proximal to Facies 3, intrusions are dyke-like, with thicknesses of 10–30 cm (Figures 9a, c). Around 10 dykes can be identified in available exposure and are of dense lava. Two families of striations are preserved on dyke faces with the S1 direction being oriented in

propagation direction (N350-65SE) and S2 being perpendicular to S1 (Figure 9c). Intrusions are found preferentially towards the unit base and are similar in form to those obtained from analogue modelling of dyke intrusion into breccia by Mathieu et al (2008). Although similar in lithology to Facies 3, dykes are slightly less rich in micro-phenocrysts and phenocrysts of olivine and clinopyroxene than Facies 1–3, with a crystallinity around 1% (Table 1).

To the east, intrusions become sill-like. These are well exposed in a disused quarry at GN-4.0;4.1 (Figure 3) and were first observed by Bonney (1912) who described the outcrop as a "lava stream catching up marl" (Figure 10a), writing that "the lava has caught up and carried along large fragments of the marl, and into that it sometimes thrusts little dykes and veins". At this outcrop, sills are around 1 m thick, can be followed into the marl for distances of 10–20 m, and are surrounded by halos of oxidized marl (Figures 10b, c). Bonney (1912) also noted that,

> "the marls, which are generally cream-coloured, are burnt to a reddish tint to a distance of from a few niches (inches) to about a yard underneath the lava, and (t)he beds are more or less bent".[4]

Sills are of dense lava identical to that of Facies 3, and some have 'a'ā-like surfaces. To the south, the sills run into a sequence of three or four 'a'ā units (Figure 10c). A 2 m wide and 1.8 m deep channel-like structure can be found associated with these units. At the marl contact, intrusions are quenched with mm-scale cooling-joints at right angles to the cooling surface. Contacts are characterized by 10 cm wide zones of powdered marl, with red-oxidized marl in a white powdery matrix beyond that. We also find 'a'ā clinker in a matrix of powdery marl (Figure 8b), attesting to the fact that the marl was poorly consolidated and easy to mechanically erode or, in the words of Bonney (1912), "catch up". All AMS-derived intrusion and flow directions are coherent with those found for Facies 3, i.e., towards the east. This is the same direction as the sense of shear and all contact orientations.

4.5. Facies 5: 'a'ā lava flow

Facies 5 is the distal part of the system and comprises two 'a'ā lava flows that extend eastwards from Facies 4 over a slope of 0.8° proximally and 0.5° distally (Figure 4). The northern (Saint Jacques) lava flow is ~3.5 km long and 289–800 m wide, and the southern (Artière-Cézeaux) flow is ~3.6 km long and 400–700 m wide. Both lava flows have thicknesses of up to ~30 m along their central axes and 15–20 m at their edges, and both are associated with cone rafts deposited on their levees (Figure 4). The two lava flows have the same density and crystal character, being dense with phenocrysts of olivine and clinopyroxene plus small (cm) xenoliths of partially melted granite (Table 1).

Proximally, Facies 5 of the Artière-Cézeaux lava flow has the form of an incipient lava channel that is ~1.2 km long and ~250 m wide (Figure 4). Undrained lava within the channel is one-to-two meters below bank (Figure 11a) and levee inner walls show signs of clast accretion (Figure 11b). The initial levees are made up of stagnated 'a'ā flow (cf. Lipman and Banks, 1987) capped by a simple rubble levee (cf. Sparks et al. 1976; Figure 11c). At outcrops along the Rue de la Résistance in Beaumont (1.5 km down channel from Facies 4), the contact between the right bank levee and the country rock is exposed (Fig. S1-1, Supplement 1). This reveals a deformed and faulted basement of marl, normally graded fluvial deposits and gelifluction lobes. The basement has been

4 Original spelling has been retained and is corrected through additions in parentheses

intruded by dense lava from the channel and is overlain by levee breccia that is a 50:50 (±10) mix of lava-derived clasts and scoria (Fig. S1-2, Supplement 1). At this and other sites down the channel section, the channel has excavated into the substrate by depths of up to ~15 m (Supplement 1).

The full flow thickness is best exposed in Beaumont at the "Basin d'Orage" (site GN5.0, Figure 3). Here the interior contains partially melted granite xenoliths and displays crude columnar jointing, with a spacing of ~1.5 m, and sits on a 3 m high zone of horizontal shear structures orientated west-east (Figure 12a). Vesicular bands and shear partings (Figure 12b), as well as ramping (Figure 12c), are present throughout the interior of Facies 5, and the basal breccia is a mixture of lava-derived clinker and scoria clasts in a fine-grained matrix (Figure 12d).

The channel feeds a ~1.4 km long zone of dispersed 'a'ā flow with a 10–20 m plug on top of a thin (~2 m) basal shear zone (Figure 12). The surface breccia has the same componentry as the breccia of Facies 3, being roughly (±10 %) an equal mix of lava clasts ('a'ā clinker and dense lava blocks) and scoria (including broken bomb fragments). Clasts can often be found coated in a powder of marl (Fig. S2-1, Supplement 2), and everywhere at the flow margins we find meter-to-decimetre sized cone chunks (e.g., Fig. S1-2, Supplement 1; see also cover map of Supplement 2).

The flow levee is best exposed in Aubière, especially down Rue Pasteur (Fig. S2-2, Supplement 2). Here, the breccia at the top of the levee is a mix of lava and scoria clasts lacking coatings of powdered marl. Towards the contact with the basement clasts become increasingly coated in marl (Fig. S2-2, Supplement 2) and pockets of breccia can be found inside the marl (Fig. S1-2, Supplement 1). Facies 5 thus lies conformably on and within the marl substrate (Figure S2-4, Supplement 2). This is consistent with the observations of Bonney (1912) who, based on his observations of the Facies 4 outcrop of Figure 10, remarked that,

> "This catching up of fragments of the underlying strata is not by any means universal, for in another quarry at some distance away, but in the same lava-stream, the latter (lava) at one part lies, with a rather even base, on laminated marls, which are discoloured and slightly indurated for a depth of a foot or so, but not otherwise affected".

Bonney's sketch of this contact resembles that currently exposed at GN5.0 (cf. Figure 10).

The flow front is best exposed at La Margeride, (Figure 3; Fig. S2-3, Supplement 2). Here the exposure is 12 m high, but the full thickness was likely greater as the surface breccia was stripped off and graded during construction of the *Université Clermont Auvergne* campus at Cézeaux (Fig. S2-5, Supplement 2). To the west (up flow) and to the north (towards the channel axis) thicknesses are up to 30 m. At the base of La Margeride a meter thickness of basal shear is exposed on top of a 1–2 m thick layer of basal breccia (Fig. S2-5, Supplement 2). The right bank lateral crust has been stripped away to the south and the basal contact is buried by cover. However, the thickness of the basal crust can be estimated from a break-in-slope about 50 m to the south and is likely 1–2 m below the base of La Margeride outcrop (Fig. S2-5, Supplement 2). The sense of shear is horizontal and to the east. Above this, we find crude columnar jointing with a spacing of ~2 m. The surface breccia has a 100% scoria content and is up to 6 m thick. It thereby represents a deci-meter scale cone raft deposited at the flow front (Supplement 2).

Ramping is apparent at all exposures, but is particularly well developed towards the top and front of the flow, as at Musée de la Vigne and La Margeride (Figure 3). At La Margeride ramps intrude the surface (Figure 12e) and extrude through the frontal breccia (Figure 12f). Ramp surfaces are striated and do not cut the columns.

Formatted: English (United States)

On top of ramp zones, the contact with the surface breccia is highly irregular, with pockets of breccia fingering around ramps (Figure 12d; Fig. S2-5, Supplement 2). At the flow front in the Creux de l'Enfer park (Figure 3), ramping causes slabs of solid lava, and fingers of breccia, to become vertically orientated (Figure 12g). As well as ramping, cone rafts and marl-coated breccia can be found all across the flow front (see Appendix S2-B of Supplement 2).

4.6. Chemistry, texture and down-system density trends

All facies of the Artière-Cézeaux lava flow are of the same composition and are trachy-basalt. They are a little poorer in SiO_2 than the Tiretaine lavas of Part 1 (Latutrie et al., 2023; Figure 13a). They are also richer in MgO and poorer in Al_2O_3 than the Tiretaine lavas (Figure 13b). Crystallinities for all five Artière-Cézeaux facies have similar values (average of 2%), and are the same as that of Grave Noire's north lava flow (Table 1). Density increases with distance from the vent (Figure 13c), so that vesicularity also decreases down system from 20–40% proximally to 3–10% distally (Table 1).

4.7. Anisotropy of Magnetic Susceptibility trends

Down-system, the AMS data show a three-field trend, each field being characterized by different degrees of anisotropy (P_j) and magnetic susceptibilities (Km). These are (Figure 14):

i) Facies 2, on the steepest slopes, have lowest P_j and Km values;
ii) Facies 5, on the shallowest slopes, have highest P_j and Km values;
iii) Facies 3 falls between these two end members.

This confirms a down-system change in flow emplacement conditions as reflected in an increase in both P_j and Km (Figure 14). Fabric alignments are also consistent with slope changes and inferred flow directions in all three facies, being:

i) SE in Facies 2;
ii) ENE in Facies 3;
iii) E in Facies 5.

Some directions are to the NE in Facies 5 due to lateral spreading (Figure 14), and some are sub-horizontal due to ramping (Appendix A).

5. The Artière-Cézeaux lava flow: Emplacement and dynamics

We use our facies analysis build an emplacement history whereby the lava flow and paleo-topography worked together. This involved emplacement of an unstable, collapsing scoria mound at the head of the steep slopes of a fault scarp. Fountaining and violent Strombolian activity fed high effusion rate lava flow down these steep slopes and into a perched pond forming behind a barrier of stalled lava at the break-in-slope at the foot of the fault scarp. The perched pond acted as an outgassing zone for the lava and thus, in turn, fed a thick, slow moving flow of dense lava that moved off across the flat-floored basin at the foot of the scarp. The basin was filled with sediment, and overlain with gelifluction lobes active in the periglacial climate 60 ka ago, and the lava excavated down into this easy-to-erode basement easy-to-erode. This sequence of events can be related to the five facies described above, where we now ascribe an origin to each facies in the same order as presented above.

5.1. Facies 1: Violent Strombolian scoria mound and cone rafts

The deposits of the Grave Noire scoria mound (Figure 5) resemble those emplaced during Etna-style fountaining (cf. Andronico et al., 2008) and violent Strombolian activity (cf. Pioli et al., 2008). Such events are typically associated with lava flows fed at effusion rates of a few tens to a few hundred cubic meters per second, being up to 40–230 m^3/s^{-1} and 350 m^3/s^{-1} for Etna and Paricutin, respectively (Ganci et al., 2012; Pioli et al., 2008). Such event also feed plumes up to 7 km high (Pailot--Bonnétat et al., 2020). Air fall from the Grave Noire plume fell onto the lava flows extending to the east to cause their surface breccia to become a mix of lava-derived clinker and air fall scoria. Advance over a scoria-covered surface also caused the basal breccia to become a mix of the two clast types.

Due to its emplacement on the crest of the Limagne fault scarp the scoria mound was extremely unstable, with large chunks sloughing off to the east in at least three major collapse events, as is apparent from the unconformities in the mound itself. Three large chunks were transported by the lava flow as "cone rafts" (cf. Németh et al., 2011) to be deposited at the flow margins at distances of up to 3 km, as is common at such systems (cf. Younger et al., 2019). Near continuous sloughing of cone material also explains the widespread proximal occurrence of debris flow deposits on, and beside, the lava flow units of Facies 2, as well as the ubiquitous presence of meter-scale cone rafts all the way to the flow front. Constant avalanching and transport of the eastern flank of the mound also inhibited crater development, explaining the absence of a crater with the cone forming a semi-circular construct on the flat, western (plateau) side of the vent.

5.2 Facies 2: Outlet channel and 'a'ā sheet flow

To the south, lava left the vent area via an outlet channel similar in form to "spillways" (Wolfe et al., 1987) active around Hawaiian cones observed on Mauna Loa (cf. Figure 57.28 of Lipman and Banks, 1987) and Kilauea (cf. Figure 1.73 of Wolfe et al., 1987). Given a flow depth (d) equal to the levee height (4 m), we estimate a mean velocity for lava flowing in a channel that is wider than it is deep from Jeffreys (1925),

$$v_{mean} = d^2 \rho g \sin(\sigma) / 8 \mu \quad (1).$$

Here, ρ is density for the outlet channel lava (2030 kg/m^3, Table 1), g is acceleration due to gravity, σ is the underlying slope (15°), and μ is viscosity. Using a viscosity for near-vent basalt at Etna of 9400±1500 Pa s (Pinkerton and Sparks, 1976), this yields velocities of 1.5–2.1 m/s. For a typical cross-sectional area of 4 m × 7 m (i.e., 28 m^2) this gives an effusion rate during brim-full flow of 40–60 m^3/s, which is consistent with our expected vent-leaving flux for lava flow fed by Etna-style fountaining (cf. Ganci et al., 2012).

The outlet channel fed thin, vesicular 'a'ā sheet flows that flooded down the steep slopes of the fault scarp. Lava flow fronts on steep slopes are notoriously unstable, and can feed near-constant hot grain flow that advance ahead of the crumbling and collapsing flow front (cf. Lodato et al., 2007). This likely explains the accumulation of lava breccia and debris flow deposits at the foot of the fault scarp in the transitional zone between Facies 2 and 3, as would continual collapses of the cone itself.

5.3 Facies 3: Perched pond

Facies 3 is consistent with a body of stagnant ponded lava that slowly cooled and outgassed in place causing the lava of this facies to be much denser of that of the 'a'ā sheet flow (Facies 2) that fed the pond. The

break-in-slope at the foot of the fault scarp would have caused lava flows descending the scarp to stall and spread. These are ideal conditions for formation of perched ponds which Wilson and Parfitt (1993) describe as:

> "uncommon but distinctive topographic features formed during some basaltic eruptions … examples include those formed during the 1968 eruption near Napau Crater (Jackson et al., 1975) and the 1974 eruption of Mauna Ulu (Tilling et al., 1987), both on Kilauea Volcano, Hawai'i. Both of these ponds are about 150 m in diameter and formed where a channelised lava flow with a relatively high volume flux encountered a region of much flatter (nearly horizontal) topography than that on which it had previously been travelling".

Thus, the change in slope caused the formation of a self-ponded flow with dimensions of 870 × 820 m and a depth of about 30 m. The stalled flow front, which was a mixture of lava-derived breccia, scoria, cone rafts and debris flow, as well as bulldozed marl, formed the barrier that contained the pond (Figure 8a). Following Wilson and Parfitt (1993), radial flow in such a pond will stop when,

$$X_p = [(E_r^4 \, K \, \mu) / (5.83 \times 10^6 \, \pi^4 \, \kappa^3 \, \rho \, g \sin(\sigma))]^{1/7} \quad (2)$$

X_p being the maximum travel distance for lava in a semi-circular pond. Here,

$$K = 3 \, [1 + 2 \, (d / w)]^2 \quad (3)$$

d and w being the depth and width of the pond, respectively (Knudsen and Katz, 1954). Given X_p (425 m), μ (9400 ± 1500 Pa s), lava thermal diffusivity (κ, 10^{-6} m^2/s, Wilson and Parfitt, 1993), density (ρ, 2740 kg/m^3, Table 1) and σ (5°), we estimate the effusion rate (E_r) that fed the pond to be 55–60 m^3/s. This is in agreement with the effusion rate calculated for lava entering the spillway at the head of the system (40–60 m^3/s), and thus feeding the pond. Velocities estimated for radial flow (from $E_r / \pi \, X_p \, d$) are, though, much lower than in the spillway being around 0.001–0.002 m/s, which is consistent with a stalling flow.

Being fed at 55–60 m^3/s, the 16.8 × 10^6 m^3 pond would have formed in around 3.5 days, although the feed could have been a result of multiple, shorter events separated by short pauses or periods of reduced supply. Such pulsed supply is suggested from the multiple scoria beds of Facies 1. This is consistent with a fountain that was sustained, but underwent cycles of waxing and waning phases, as is apparent from the repeated normal grading. Pulsed supply is also consistent with the multiple sheet flow units of Facies 2. If each thin 'a'ā unit on the fault scarp above the pond is equal to one supply event, then there were at-least 18 events, and maybe as many as 40.

The time (t) needed to solidify a stagnant lava pond of depth d can be estimated from:

$$d = \lambda \sqrt{(\kappa \, t)}, \quad (4)$$

in which λ is a dimensionless scaling value with a value of 0.876 (Turcotte and Schubert, 2002). For a ~30 m deep pond this gives a cooling time of 60–65 years. During slow cooling of this stagnant pond, columns formed (cf. Peck and Minakami, 1968), and became deformed down slope to the east (Figure 8a).

5.4. Facies 4: Brecciated barrier and seeps

Proximal to the pond, the barrier material is derived from the lava flow itself. That is, it is a 50:50 mix of scoria and clinker. However, with distance the barrier becomes an increasing mix of lava and marl, suggesting that the flow bulldozed into the soft, unconsolidated marl. The barrier and the marl was then injected by lava in the form of dykes proximal to the pond, transitioning to sills with distance; with the hot intrusions locally oxidizing the marl into which they were injected. Intrusions are generally towards the base of the barrier where

pressures would have been highest, and fed ‘a‘ā flows that exited the barrier at its base as “seeps” (cf. Patrick and Orr, 2012). Channels leaving the barrier also excavated downwards into the easily-erodible marl to form “excavated debris levees” (cf. Calvari et al., 2005) and injected lava into the marl to form sills in the distal barrier facies (Figure 10).

Lava involved in the intrusions was degassed, high-density lava from the pond (Table 1). We estimate the pressure, P, for an intrusion from the base of the lake to be:

$$P = d\ \rho\ g = 30\ m \times 2580\ kg/m^3 \times 9.8\ m/s^2 = 0.7\ MPa \quad (5)$$

Following Kauahikaua et al. (1996) we can use P to estimate the volume flux through a conduit of radius r from

$$E_r = (\pi\ r^4 / 8\ \mu)\ \Delta P/\Delta x \quad (8)$$

Given a barrier width of around 500 m we obtain $\Delta P/\Delta x$ of 1.7 kPa/m. This, for a degassed lava viscosity of 10^4 Pa s (Harris et al., 2005) and a dyke radius of 0.5 m, yields E_r of 0.004 m^3/s per dyke. At least ten dykes were active so the total seep flux was likely >0.04 m^3/s. To the north and south, the barrier was also cut, or overflowed, by channelized lava. The dimensions of the channel to the south of the barrier (2 × 1.8 m) gives a velocity of 0.1 m/s and an effusion rate of 0.2 m^3/s. Thus, multiple low effusion rate “seep” sources, plus overflows and breakouts, fed the Facies 5 lava flow that extended across the nearly flat slopes of the Limagne basin.

5.5. Facies 5: Seep-fed ‘a‘ā

Having spent time in the perched pond, the lava of Facies 5 was nearly completely outgassed. The multiple seep sources organized themselves into a single, broad channel that fed a simple, single lava flow unit (cf. Walker, 1972). The dense and viscous state of the lava meant that flow was plug dominated. A basal shear zone thickness of 1–2 m, and a unit thickness of 20–30 m, gives a plug height of 18–28 m. Following Hulme (1974), we can use the plug height (h_0) to estimate yield strength (τ_0):

$$\tau_0 = h_0\ \rho\ g \sin(\sigma) \quad (9)$$

For a density of 2700 kg/m^3 (Table 1) and slope of 0.5°, this gives τ_0 of 4.2–6.5 × 10^3 Pa, which is relatively high for basaltic lavas, which tend to have yield strengths of a few hundred Pascal (cf. Fink and Zimbleman, 1986; Wadge and Lopes, 1991). This attests to the degassed and rheologically evolved state of the Facies 5 lava flow. We can estimate the velocity at the base of the plug from:

$$v_{plug} = (d^2 - h_0^2)\ \rho\ g\ \sin(\sigma) / 3\ \mu \quad (10)$$

Using a viscosity of 6 × 10^6 Pa s for outgassed, distal lava (Moore, 1987) we obtain a velocity of 0.001 m/s. Because the mass of the plug moves at the same velocity as the shear zone that carries it (cf. Cigolini et al., 1984), this would have been the velocity at which the bulk of the flow moved. We thus have a plug-dominated flow with the non-deforming plug being transported by a thin basal layer of shearing lava, which is closer to the emplacement mode of a silicic lava flow than a typical channel-fed basaltic ‘a‘ā system (cf. Harris et al., 2002; Latutrie et al., 2017; Prival et al., 2022). Given the extended cooling time for the source of the Facies 5 lava (i.e., the perched pond) supply by slow but steady seeping of high viscosity and yield strength lava through the barrier could, potentially, have been sustained for tens of days; even years.

For a flow width of 400–700 m, which is thinner distally (30 m) than proximally (20 m), a velocity of 0.001 m/s translates to an effusion rate of 14–17 m^3/s. At these velocities and effusion rates, emplacement time (i.e., time needed to extend 3.6 km or build a flow volume of 49.5 × 10^6 m^3) would have been around 40 days.

Again, this was from multiple seeps, but also likely from failure of part of the barrier containing the Facies 3 pond, as witnessed by the dominance of cone chunks and material with evidence of substrate interaction at the flow front. We interpret these the cone chunks as being parts of the barrier carried to the flow front by the lava initially breaking out from the pond. Excavation and intrusion of the marl by the Facies 5 channel, as well as coverage of clasts comprising the flow front breccia in marl (Supplements 1 and 2), indicate high degrees of mechanical erosion in the marl substrate. Excavation was to a depth of around 15 m to create a channel partially set into the substrate (Fig. S2-4, Supplement 2) and with a time-averaged excavation rate of 30–40 cm per day.

5.6. The Artière-Cézeaux perched pond and lava flow system: emplacement model and Hawaiian analogues

Although debris avalanching contributed to cone rafts transported by the flow, as well as a mixed covering of cone-, lava- and air-fall-derived material, the Artière-Cézeaux system cannot be classed as a debris avalanche, as considered by Goër de Herve et al. (1993) and Boivin et al. (2017). Debris avalanche is a convenient class into which such a complicated facies can be placed, but such a classification overlooks the complex emplacement conditions of a lava flow advancing not just over a highly-erodible substrate, but also over a topography with abrupt changes in slope. The system instead is a lava flow → perched pond → lava flow sequence (Figure 15a). As summarized in Table 3, the establishment of this morphological system[5] resulted from the interplay of effusion rate and topography. As part of the associated cascading system[6] fountain-fed supply at high effusion rates onto steep slopes led, proximally, to fast moving sheet flow. On reaching the break-in-slope to flatter ground, flow stalled and spread to create a perched pond behind a barrier of its own making. The barrier was in turn intruded and overflowed by pond lava to feed flow onto the near-flat land beyond the barrier (Figure 15b). The pond acted as a holding zone in which lava degassed so that flow fed by the pond was dense, rheologically evolved and, consequently, very slow moving. The barrier also modulated flow, so that lava exited the pond at a much lower volume flux, and over a much longer time scale, than that at which it entered the pond (Table 3). Topographically and dynamically the resulting process-response system[7] is that given in Figure 15 and Table 3.

The pond and seep sequence apparent down the Artière-Cézeaux system appears similar to down-system flow behaviour witnessed on Kilauea (cf. Patrick and Orr, 2012). During perched pond formation at Kilauea in 2008 ponds 200 m in diameter became active behind porous barriers of flow breccia (Figure 16). These remained active for periods of several days (Patrick and Orr, 2012), feeding flow by overflow and from "seeps" opening at the base of the barrier (Figure 16). In this regard, a seep can be viewed as a secondary vent fed by lava exiting the pond via intrusion of the barrier, as documented by us at the Artière-Cézeaux system (cf. Figure 15b). As at Kilauea, we also record barrier failure leading to flow from the north of the Artière-Cézeaux pond (Figure 15a). At Artière-Cézeaux, breakout flow and seep-fed lava coalesced to feed the final segment of the process-response system (Figure 15b). We find a similar situation for the north flow (Figure 4), where we

[5] Senso Dury (1981): *A system defined in terms of attributes (such as geometry, structures, colors, fabrics and textures), and arrangement of those attributes*.
[6] Senso Dury (1981): *A system that considers complex inputs/outputs of energy (E) and mass (m), and which provides for storage of E and m while allowing for delays between total input & output of E and m.*
[7] Senso Dury (1981): *A combination of at least one morphological system and one cascading system, where the character of the morphological system changes in response to cascading inputs.*

also see evidence for formation of a perched pond at the break-in-slope from steep to flat (Figure 15c). This northern pond, likewise, fed a denser, thicker, more viscous unit to (i) create a barrier in the Tiretaine valley (Figure 15c), and (ii) spread onto the flat land of the basin (Table 3).

5.7. Comparison of the Tiretaine and Artière-Cézeaux systems

A comparison of the facies associated with the Tiretaine lava flow system of Part 1 (Latutrie et al., 2023), and Artière-the Cézeaux system of Part 2, and their relation with flow dynamics and changes in slope, is given in Table 3. We see that the two cases are inverse in terms of slope. The proximal portion of the Tiretaine lava flow field was built on gentle, with flow then moving onto steep slopes. Instead, the Artière-Cézeaux lava flowed down steep slopes and out onto a near-flat plain. The same is true of effusion rates, which were high proximally for the Artière-Cézeaux lava flow but low for the Tiretaine. Instead, effusion rates were low distally for the Artière-Cézeaux lava flow, but high for the Tiretaine. The gentle proximal slopes of the Tiretaine system allowed slow inflation of a pāhoehoe flow field. Instead, a near-vent steep slopes and break-in-slope at the Grave Noire caused the Artière-Cézeaux lava to flood down these slopes to stall quickly and pond. The effect of both the inflated pāhoehoe flow field of the Tiretaine and the pond of Artière-Cézeaux was the same; they stored lava to allow outgassing and modulation of the down system flux. For the Tiretaine, failure of the pāhoehoe flow front suddenly released a stored volume of dense lava to feed high effusion rate, valley-contained flow. For the Artière-Cézeaux system, slow leaking of a breccia barrier fed effusion of dense lava at low rates. Time scales of emplacement were thus also inverted proximally and distally between the two systems (Table 3).

The combination of down flow changes in slope and effusion rate led to a characteristic arrangement of facies for the two systems (Table 3). For the Artière-Cézeaux these were related to a down-system evolution in the morphological system of:

- channelized flow → storage → channelized flow

For the Tiretaine it was:

- storage → channelized flow → storage

Both process-response systems have a barrier in common. However, in the case of the Artière-Cézeaux lava flow the barrier was generated by stalling of the flow itself. Instead, for Tiretaine lava flow the barrier was a dam of Grave Noire lava. These barriers respectively resulted in the creation of medial and distal storage zones in the two systems.

5.8 Inversion of relief and geoheritage

Emplacement of the Artière-Cézeaux lava flow system displaced the drainage to the south where, proximally (to the south of Boisséjour) the new stream course used the easily erodible lateral breccia of the pond (Figure 15c). Here, as at the Tiretaine system of Part 1 (Latutrie et al., 2023), the stream cut a 5–10 m deep gulley floored with rounded pebbles and boulders of granite and basalt. If we include the 26 m thickness of the lava unit that fills the paleo-valley here, this is 30–40 m of erosion since the emplacement of the system. With preferential erosion of the down flow breccia barrier over the massive interior, the perched pond today represents a lobate plateau of inverted relief bounded to the east and south by steep slopes and cliffs (Figure 15c).

Where the flow system extends out onto the Limagne plain, inversion of relief has already progressed towards the final phase of inversion, where the paleo-valley of the Artière is, today, a broad flat-topped plateau

bounded to the south by the new valley of the Artière (Figure 4; Supplement 1). Here, the resistant lava flow cap has protected the underlying sediments from erosion, so that the plateau surface stands above the valley floor to the south by up to 15–30 m. This gives at least 15 m of erosion of the sediments surrounding the lava flow in the 60 ky since its emplacement. This contrasts with the case of the Tiretaine (Part 1, Latutrie et al., 2023) which was emplaced in a less erodible terrain, and is still at the stage 1 of the inversion process (stream displacement), the granitic host topography being less easy to erode than the sediments surrounding the Artière-Cézeaux system.

Inversion of relief has already been exploited by man, where the town of Beaumont, as well as the village of Boisséjour, have been built on the stable and flat surfaces of the basalt plateaux, a surface which also protects the town from flooding (Figure 4). This region is also known for the Cotes d'Auvergne wine (France, 2008: p. 125), and vineyards are sited on the south flanks of such inverted relief (Auvergne Patrimone, 2004). This has been the case around the town of Aubière on the south flank of the Cézeaux plateaux (Figure 4). Here, the basalt was used for the excavation of wine cellars in the 18th and 19th centuries (Auvergne Patrimone, 2004), and these still exist next to roads that climb up the south side of the Cézeaux plateau and expose the geology on which they rely (Supplement 2). Here, the museum of the vine and wine (le museé de la vigne et du vin, Figure 3) is aptly located. Our work will help create more detailed outcrop inventories for the Clermont Auvergne Metropole (cf. Vereb et al 2020) and will aid in the protection of such sites to the benefit of geotourism. Not only are they valuable as geological sites of scientific excellence, but they also provide outstanding examples of how land-use systems develop around geologic events.

7 CONCLUSION

In effusive systems perched pond formation has been observed and described since the nineteenth century (Dana 1849), but only on Kilauea (e.g., Jackson et al. 1975; Tilling et al. 1987; Wilson and Parfitt 1992). Based on these observations, Wilson and Parfitt (1992) proposed an emplacement model for perched ponds that highlighted the role of a break-in-slope, from steep to flat, in pond formation. The break-in-slope reduces the lava flow velocity, causes radial dispersion and increases heat loss, producing thick crusts on the sides and fronts of the flow, while the central part continues to be fed by hot and fluid lava from the source, which in our case was a spillway from a fountaining vent. Our observations at the Grave Noire thus show that such features can be found in any flow system at which high effusion rate flow crosses a boundary between high and low slopes over a short distance.

Creation of a preched pond → seep-fed flow system requires a down flow topographic change from steep to gentle slopes. In Part 1 (Latutrie et al., 2023), we analysed the reverse case where there was a change from gentle to steep slopes down the Tiretaine lava flow system. At the Tiretaine system, we witnessed an event that had time scales and effusion rates that were the reverse of those considered here. Both systems have active analogues that can be taken from Hawaii, but for which the exposure available in our systems allows access to hidden, interior processes that are not apparent in active cases. After the Tiretaine system, the Artière-Cézeaux lava flow system is thus a second outstanding example of an effusive system that has its source in a UNESCO world heritage site. In the Artière-Cézeaux case, outcrop exposure of a perched pond–seeping system fed by fountain-fed sheet flow via a spillway is preserved. Thus, as in the conclusion of Part 1 (Latutrie et al., 2023), we stress the value of studies such as this in advancing and linking understanding of volcanic processes, as well as

in supporting inventories for geoheritage-orientated initiatives and outreach. In this regard, the Grave Noire is a classic example of an effusive system erupted onto steep terrain above a plain.

8 Acknowledgements

This research was financed by the Agence National de la Recherche through the project LAVA (Program: DS0902 2016; Project: ANR-16 CE39-0009). The work was also carried out under the UNESCO International Geoscience Programme project 692 'Geoheritage for Resilience'. This is ANR-LAVA contribution no. XX and Laboratory of Excellence ClerVolc contribution no. XX. We are grateful to the comments and suggestions of the two reviewers, James Kauahikaua and Steve Self, and to Thor Thordarson whose comments from Part 1 (Latutrie et al., 2023) were carried over into improving Part 2. We also thank Sonia Calvari for her attentive and efficient editorial handling of the paper pair.

AUTHOR CONTRIBUTION

AH, BL, BV, ES, MF, LG, EZ, EM and FN completed all fieldwork, mapping and sampling between 2011 and 2022. AH lead final write up, with all co-authors. BL and ES performed all textural and petrological analyses under the guidance of LG in 2016 and 2020-2021, and all chemical analyses under the guidance of EM and FN. EZ completed all AMS measurements. BL completed sampling, analyses and mapping as part of a contract funded by ANR-LAVA (as managed by AH) during 2020-2021.

DATA AVAILABILITY

All textural and chemical data are freely available via the DynVolc (http://wwwobs.univ-bpclermont.fr/SO/televolc/dynvolc/) observation system and database managed by LG

REFERENCES

Andronico, D., Cristaldi, A. and Scollo, S., 2008. The 4–5 September 2007 lava fountain at south-east crater of Mt Etna, Italy. J Volcanol Geotherm Res, 173: 325-328.

Auvergne Patrimone, 2004. Le vigne et le vin en Auvergne. Chamina (Clermont Ferrand, France), 143 P.

Boivin, P., Besson, J.C., Briot, D., Deniel, C., Gourgaud, A., Labazuy, P., de Larouzière, F.D., Langlois, E., Livet, M., Médard, E., Merciecca, C., Mergoil, J., Miallier, D., Morel, J.M., Thouret, J.-C. and Vernet, G., 2017. Volcanology of the Chaîne des Puys. In: P.N.R.l.C.d.P. (Ed.) (Editor), Cart. Fasc. 6e édition: 200p, 1/25000.

Bonney, T.G., 1912. Volcanoes: Their structure and significance. John Murray (London): 379 p

Borde, P. and Rudel, A., 1939. Note sur une des grottes de la coulée de Gravenoire, 97 p.

Bournet, G., 1957. Observations nouvelles sur le volcan de Gravenoire, 87 p.

Calvari, S., Spampinato, L., Lodato, L., Harris, A.J.L., Patrick, M.R., Dehn, J., Burton, M.R. and Andronico, D., 2005. Chronology and complex volcanic processes during the 2002–2003 flank eruption at Stromboli volcano (Italy) reconstructed from direct observations and surveys with a handheld thermal camera. J Geophys Res: Solid Earth, 110, B02201, doi:10.1029/2004JB003129.

Formatted: French (France)

Formatted: French (France)

Cas, R.A.F. and Wright, J.V., 1987. Volcanic successions modern and ancient: A geological approach to processes, products and successions. Springer.

Cigolini, C., Borgia, A., and Castertano, L., 1984, Intracrater activity, aa-block lava, viscosity and flow dynamics: Arenal volcano, Costa Rica: Journal of Volcanology and Geothermal Research, v. 20, 155–176.

Dana, J.D., 1849, United States Exploring Expedition, vol. X Geology, Philadelphia, C. Sherman, 756 p.

Dury, G.H., 1981. An Introduction to Environmental Systems, Heinemann Educational Books (Exeter, NH): 306 p.

France, B., 2008. Grand Atlas des Vignobles de France. Solar Editions (Paris, France), 322 p.

Fink, J.H. and Zimbelman, J.R., 1986. Rheology of the 1983 Royal Gardens basalt flows, Kilauea volcano, Hawaii. Bull Volcanol, 48: 87-96.

Foucher, M., 2013. Stage de Terrain sur le Puy de Gravenoire, Université Blaise-Pascal, 27 pp.

Ganci, G., Harris, A.J.L., Del Negro, C., Guéhenneux, Y., Cappello, A., Labazuy, P., Calvari, S. and Gouhier, M., 2012. A year of lava fountaining at Etna: volumes from SEVIRI. Geophys Res Lett, 39.

Garde, G., 1942. Les anciens volcans de Gravenoire et de Charade (pres de Clermont-Ferrand). Bull Soc Géol France, 5: 261-270.

Glangeaud, P., 1901. Monographie du volcan de Gravenoire près de Clermont-Ferrand. Béranger.

Goër De Herve, A., Camus, G., Miallier, D., Sanzelle, S., Falguères, C., Fain, J., Montret, M. and Pilleyre, T., 1993. Le puy de Gravenoire et ses coulees, dans l'agglomeration de Clermont-Ferrand (Massif central francais); un modele inhabituel d'avalanche de debris, declenchee par une eruption strombolienne en climat periglaciaire. Bull Soc Géol France, 164: 783-793.

Guettard, J.E., 1752. Mémoire sur quelques montagnes de la France qui ont été des volcans.

Harris, A.J.L., Flynn, L.P., Matías, O. and Rose, W.L., 2002. The thermal stealth flows of Santiaguito dome, Guatemala: Implications for the cooling and emplacement of dacitic block-lava flows. Geol Soc Am Bull, 114: 533-546.

Harris, A.J.L., Flynn, L.P., Matias, O., Rose, W.L. and Cornejo, J., 2004. The evolution of an active silicic lava flow field: an ETM+ perspective. J Volcanol Geotherm Res, 135: 147-168.

Harris, A.J.L., Bailey, J., Calvari, S. and Dehn, J., 2005. Heat loss measured at a lava channel and its implications for down-channel cooling and rheology. Geol Soc Am - Spe Pap, 396: 125.

Hulme, G., 1974. The interpretation of lava flow morphology. Geophys J Inter, 39: 361-383.

Jackson, D.B., Swanson, D.A., Koyanagi, R.Y. and Wright, T.I., 1975. The August and October 1968 East Rift Eruptions of Kilauea Volcano, HawaiiI. US Geol Surv Prof Pap 890: 33p.

Jeffreys, H., 1925. The flow of water in an inclined channel of rectangular section. The London, Edinburgh, and Dublin Philosophical Magazine and Journal of Science, 49: 793-807.

Kauahikaua, J.P., Mangan, M., Heliker, C. and Mattox, T., 1996. A quantitative look at the demise of a basaltic vent: The death of Kupaianaha, Kilauea Volcano, Hawai'i. Bull Volcanol, 57: 641-648.

Formatted: French (France)

Knudsen, J.G., and Katz, D.L., 1954. Fluid dynamics and heat transfer. McGraw-Hill (New York): 243 p.

Latutrie, B., Harris, A.J.L., Médard, E. and Gurioli, L., 2017. Eruption and emplacement dynamics of a thick trachytic lava flow of the Sancy volcano (France). Bull Volcanol, 79: 4.

Le Maitre, R.W., Streckeisen, A., Zanettin, B., Le Bas, M.J., Bonin, B., Bateman, P., Bellieni, G., Dudek, A., Efremova, S., Keller, J., Lameyre, J., Sabine, P.A., Schmid, R., Sorensen, H. and Woolley, A.R., 1989. Igneous rocks: A classification and glossary of terms. Recommendations of the international union of geological sciences subcommission on the systematics of igneous rocks. Cambridge University Press. p 256.

Lecoq, H., 1867. Les époques géologiques de l'Auvergne. Baillière et fils.

Lipman, P.W. and Banks, N.G., 1987. Aa flow dynamics, Mauna Loa 1984. US Geol Surv Prof Pap, 1350: 1527-1567.

Lockwood, J. and Lipman, P., 1980. Recovery of datable charcoal beneath young lavas: lessons from Hawaii. Bull Volcanol, 43: 609-615.

Lodato, L., Spampinato, L., Harris, A.J.L., Calvari, S., Dehn, J. and Patrick, M., 2007. The morphology and evolution of the Stromboli 2002–2003 lava flow field: an example of a basaltic flow field emplaced on a steep slope. Bull Volcanol, 69: 661-679.

Maccaferri, F., Acocella, V. and Rivalta, E., 2015. How the differential load induced by normal fault scarps controls the distribution of monogenic volcanism. Geophys Res Lett, 42: 7507-7512.

Mathieu, L., De Vries, B.V.W., Holohan, E.P. and Troll, V.R., 2008. Dykes, cups, saucers and sills: Analogue experiments on magma intrusion into brittle rocks. Earth Planet Sci Lett, 271: 1-13.

Merle, O. and Michon, L., 2001. The formation of the West European Rift; a new model as exemplified by the Massif Central area. Bull Soc Géol France, 172: 213-221.

Moore HJ (1987) Preliminary estimates of the rheological properties of 1984 Mauna Loa lava. UGSG Prof Pap 1350:1569–1588

Németh, K., Risso, C., Nullo, F. and Kereszturi, G., 2011. The role of collapsing and cone rafting on eruption style changes and final cone morphology: Los Morados scoria cone, Mendoza, Argentina. Open Geosciences, 3: 102-118.

Ollier, C.D., 1988. Volcanoes. Second Edition. Basil Blackwell, Oxford.

Pailot-Bonnétat, S., Harris, A.J.L., Calvari, S., De Michele, M. and Gurioli, L., 2020. Plume Height Time-Series Retrieval Using Shadow in Single Spatial Resolution Satellite Images. Remote Sensing, 12: 3951.

Patrick, M.R. and Orr, T.R., 2012. Rootless shield and perched lava pond collapses at Kīlauea Volcano, Hawai'i. Bull Volcanol, 74: 67-78.

Peck, D.L. and Minakami, T., 1968. The formation of columnar joints in the upper part of Kilauean lava lakes, Hawaii. Geol Soc Am Bull, 79: 1151-1166.

Pinkerton, H. and Sparks, R.S.J., 1976. The 1975 sub-terminal lavas, Mount Etna: a case history of the formation of a compound lava field. J Volcanol Geotherm Res, 1: 167-182.

Pioli, L., Erlund, E., Johnson, E., Cashman, K., Wallace, P., Rosi, M. and Granados, H.D., 2008. Explosive dynamics of violent Strombolian eruptions: the eruption of Parícutin Volcano 1943–1952 (Mexico). Earth Planet Sci Lett, 271): 359-368.

Pommerol, F., 1880. L'âge du volcan de Grave-noire. AFAS, 9è session, Reims, (1881): 72-78.

Ross, P.-S., Giroux, B. and Latutrie, B., 2021. Precision and accuracy of modal analysis methods for clastic deposits and rocks: A statistical and numerical modeling approach. Geosphere.

Saubin, E., 2014. Etude dynamique, texturale et rhéologique de laves mises en place sur une pente forte: Exemple de Gravenoire dans la chaîne des Puys, Université Blaise-Pascal, 26 pp.

Scrope, G.J.P., 1858. The geology and extinct volcanos of central France.

Sparks, R.S.J., Pinkerton, H. and Hulme, G., 1976. Classification and formation of lava levees on Mount Etna, Sicily. Geology, 4: 269-271.

Tilling, R.I., Christiansen, R.L., Duffield, W.A., Endo, E.T., Holcomb, R.T., Koyanagi, R.Y., Peterson, D.W. and Unger, J.D., 1987. The 1972–1974 Mauna Ulu eruption, Kilauea Volcano: an example of quasi-steady-state magma transfer. US Geol Surv Prof Pap, 1350: 405-469.

Turcotte, D.L. and Schubert, G., 2002. Geodynamics. Cambridge university press.

van der Plas, L. and Tobi, A.C., 1965. A chart for judging the reliability of point counting results. Am J Sci, 263: 87-90.

Vereb, V., Van Wyk de Vries, B., Guilbaud, M.-N. and Karátson, D., 2020. The urban geoheritage of Clermont-Ferrand: from inventory to management. Quaestiones Geographicae, 1(ahead-of-print).

Wadge, G. and Lopes, R.M.C., 1991. The lobes of lava flows on Earth and Olympus Mons, Mars. Bull Volcanol, 54: 10-24.

Walker, G.P.L., 1972. Compound and simple lava flows and flood basalts. Bull Volcanol, 35(3): 579-590.

Wilson, L. and Parfitt, E.A., 1993. The formation of perched lava ponds on basaltic volcanoes: the influence of flow geometry on cooling-limited lava flow lengths. J Volcanol Geotherm Res, 56: 113-123.

Wolfe, E.W., Garcia, M.O., Jackson, D.B., Koyanagi, R.Y., Neal, C.A. and Okamura, A.T., 1987. The Puu oo eruption of Kilauea volcano, episodes 1–20, January 3, 1983, to June 8, 1984. US Geol Surv Prof Pap, 1350: 471-508.

Younger, Z.P., Valentine, G.A. and Gregg, T.K.P., 2019. 'A'ā lava emplacement and the significance of rafted pyroclastic material: Marcath volcano (Nevada, USA). Bull Volcanol, 81: 1-15.

FIGURE CAPTIONS

Figure 1 Examples of lava flows running from steep slopes to low inclines. A. the two cases studied, case 1 (Part 1, Latutrie et al., 2023) when a lava flows from flat to steep, and case 2 (this paper) where a lava moves from steep slopes to flatter land. B. Block diagram depicting the two cases. There are two scenarios to which case 2 could apply, (i) lava erupting from a vent at the top of a steep scarp, and (ii) where a vent opens on the edge of a steep valley. C. example from Momotombo volcano (Nicaragua) of lavas descending a steep slope and spreading on flat ground to form ponds that are breached by breakouts. D. Example from Concepción volcano

(Nicaragua) with thin flows on steep slopes feeding a pond at the base of the slope, which in turn feed breakout lobes. E. An escarpment on the south flank of Kilauea (Hawai'i) with thin flows on steep slopes, that stall, spread and pond on the flatter area below.

Figure 2 Location of the Chaîne des Puys (A) and evolution of Grave Noire geological maps. B) Geological map from Glangeaud (1901) displaying many small scoria cones in association with lava flows; C) Geological map from Garde (1942) who considered that all lava flows were generated by Grave Noire and were able to disrupt and carry parts of the Strombolian edifice; D) Geological map from Goër de Herve et al. (1993) highlighting small scoria cones (stipple), associated with lava flows (wiggly line fill) and a debris avalanche deposit (black pattern) on granite (crosses), marl and sediment (white and dashed line fill); E) Geological map of Boivin et al. (2017) displaying scoria rafts (mapped as brown with white dots) on the top of Grave Noire lava flows.

Figure 3 Map displaying the location of all Grave Noire outcrops visited, pictures used for facies descriptions on figures, plus samples used for textural/geochemical analyses and AMS measurements. Note that the red number 1 corresponds to northwest quarry and the red number 2 to the east quarry of the Grave Noire scoria mound.

Figure 4 Geological map of the Grave Noire lava flow field with details of the five facies defined for the Artière-Cézeaux lava flow. Map is the result of the mapping and sampling of Figure 3.

Figure 5 Facies 1: the Grave Noire scoria mound and cone chunks. A) Exposure of the cone interior in the northwest quarry, with bedding detail as enlarged in (B). C) Exposure of the cone interior in the east quarry, with bedding detail as enlarged in (D) showing at-least nine normally graded beds over a height of around 10 m. E) Cut face of sample GN-1 which come from the dense dyke in the east quarry showing entrained scoria. F) Scoria pile on the north side of the lava flow at “La Châtaigneraie”. See Figure 3 for the location of the pictures, samples and quarries (red numbers).

Figure 6 Facies 2: stacked ‘a‘ā lava flows. A) Log of exposed flow with B) a single unit in the forest above Boisséjour and C) detail of the vesicular interior (sample GN-2.5). See Figure 3 for the location of the pictures and samples.

Figure 7 Facies 2: outlet channel. A) Left bank levee and overflow units, with detail of B) overflow units, C) their interiors with mixed, entrained scoria, and D) the vesicularity of the overflow lava core of sample GN-2.0 (cf. Figure 6c which has a similarly vesicular character). See Figure 3 for the location of the pictures and samples.

Figure 8 Facies 3: ponded lava. Main outcrops and structures with A) the full thickness of the ponded unit as exposed at a quarry at the eastern entry to the village of Boisséjour, and B) close-up view of the surface breccia showing a mix of rounded ‘a‘ā clinker and broken scoria. See Figure 3 for the location of the pictures.

Figure 9 Facies 4: lava-scoria breccia and marl barrier. A) outcrop in a building foundation excavation on the NW side of Boisséjour (exposure no longer available) showing dense lava intrusions in the brecciated unit. B) close-up of the breccia showing lava-derived and scoria fragments in a matrix of powdered marl. C) Close-up of an intrusion showing surface striations and the S1/S2 orientations. See Figure 3 for the location of the pictures.

Figure 10 A) Sketch of Bonney (1912) of the north face of the quarry in Facies 4 (lava-scoria breccia and marl barrier) showing a "lava stream catching up marl". B) Photo of the west face showing sills and ‘a‘ā flows in marl, C) Sketch and photos of the east face showing sills in marl extending from ‘a‘ā units, D) east face during winter when breccia was covered with snow. E) A view of the east face in the summer showing layers of massive lava (‘a‘ā flow interiors) and their brecciated tops and bottoms. See Figure 3 for location of pictures.

Figure 11 Facies 5: ‘a‘ā lava channel and levees. A) Schematic of a typical lava channel (not at scale) and associated levees. B) Accretionary levee exposed along the Ave. des Mont Dore, Beaumont, and C) rubble levee exposed at Saint-Jacques. See Figure 3 for the location of the pictures

Figure 12 Schematic of an ‘a‘ā lava flow in cross-section after Lockwood and Lipman (1980) with all of the components observed in Facies 5 (degassed, sheared ‘a‘ā lava flow). A) Core near the front at "La Margeride" displaying xenoliths of granite, B) sub-horizontal shearing structures and vesicle bands, C) ramps, D) basal breccia displaying sub-rounded clinkers, ramp structures extruding through the flow front E) and F) surface breccia, G) flow front breccia displaying mix of lava-derived and scoria fragments. See Figure 3 for location of the pictures.

Figure 13 A) TAS diagram derived from Le Maitre (1989) highlighting that the Grave Noire lavas are Trachy-basalts (Table 2), B) Al_2O_3 vs MgO Harker diagram displaying that Artière/Cézeaux sample and field of the Tiretaine samples of Part 1 (Latutrie et al., 2023), C) density versus distance to GN-1.0 down the Artière/Cézeaux system (data from Table 1). Literature data are from the LMV database as used for Boivin et al. (2017).

Figure 14 Anisotropy of magnetic susceptibility data for each site grouped according to facies. The principal susceptibility axes are plotted on an equal-area, lower-hemisphere projection. Symbols: square = k_1 direction; triangle = k_2 direction. Data are also plotted as down-system change in slope, P_j and Km. All change systematically down system and are consistent with (i) sheet flow to the ESE for lava on the steep slopes of the fault scarp (facies 2); (ii) deformation to the ENE in lava ponding at the base of the fault scarp and intrusion of / flow through the pond barrier (facies 3&4); and (iii) flow to the east on the quasi-flat plain to beyond the pond (facies 5: degassed, viscous lava fed by the pond).

Figure 15 A) The Grave Noire lava flow system in plan and section, focusing on the outlet channel, ‘a‘ā sheet flow, perched pond and intruded barrier showing the components of a perched pond – seep system, B) West-east cross-section of the Grave Noire flow system (see Figure 3 for the location of the section) and C) North-south

cross-section passing through the Tiretaine valley to the north up to the Artière valley to the south (see Figure 3 for the location of the section).

Figure 16 Photos and infrared images of perched ponds and seeps active in the Royal Gardens area of Kilauea on 31 January 2008 (Photographs from T. Orr and thermal camera image from M. Patrick, both U.S. Geological Survey Hawaiian Volcano Observatory).

Appendix A. Sample-derived magnetic fabrics by facies